Phage-based microbiome manipulation elucidates interactions within community context

Tomas Hessler[1,2,3]*, Dawn M. Chiniquy[3], Benjamin A. Adler[1], Jordan Hoff[1], Eliana Tucker[3], Robert Huddy[4], Rohan Sachdeva[1], Shufei Lei[1], Susan T. L. Harrison[5,6,7], Rodolphe Barrangou[8], Spencer Diamond[1], Adam M. Deutschbauer[3,9], Jillian F. Banfield[1,2,3,10] *

[1]The Innovative Genomics Institute at the University of California, Berkeley, California, USA
[2]The Department of Earth and Planetary Science, University of California, Berkeley, California, USA
[3]Environmental Genomics and Systems Biology Division, Lawrence Berkeley National Laboratory, Berkeley, CA, USA
[4]Research Office, Faculty of Health Sciences, University of Cape Town, Cape Town 7700, South Africa
[5]The Center for Bioprocess Engineering Research, University of Cape Town, South Africa
[6]The Future Water Institute, University of Cape Town, South Africa
[7]Faculty of Engineering, Architecture & IT, University of Queensland, St Lucia, Australia
[8]North Carolina State University, Raleigh, USA
[9]Department of Plant and Microbial Biology, University of California, Berkeley, California, USA
[10]Department of Microbiology, Biomedicine Discovery Institute, Monash University, Melbourne, VIC, Australia

*Corresponding authors: tomas.hessler@berkeley.edu, jbanfield@berkeley.edu

Abstract

Testing microbial interaction hypotheses remains a major challenge in microbiome research. Bacteriophages have the potential to probe organism-organism interactions within complex microbiomes, yet are rarely used for this purpose. Here, we isolated nine narrow host range phages that replicate in several ecologically important *Variovorax* species. As *Variovorax* CL14 degrades the plant root-stunting hormone auxin, we used phages to eliminate *V.* CL14 from a rhizosphere consortium and reestablished the stunted root phenotype. We used three of the phages to deplete another *Variovorax*, SCN45, from complex communities to test correlation network-based hypotheses of thiamine interdependencies. Genome-resolved metagenomics revealed that specific taxa decreased in relative abundance following *Variovorax* depletion and could be rescued by thiamine supplementation. Thus, we confirmed thiamine production as the mechanistic basis for interdependence. These experiments lay the foundation for research that employs wildtype and engineered phages to test interaction hypotheses and for targeted microbiome manipulation.

Introduction

Microorganisms form the foundation of food webs, and profoundly influence the health of plants, humans, and other animals on a global scale. Yet microorganisms rarely function in isolation, and instead form complex communities in which a multitude of interactions shape its structure (Pacheco et al., 2019, Ma et al., 2020, Kost et al., 2023, Clegg & Gross, 2025).

Complex microbial communities have long been studied using metagenomics (Tyson et al., 2004), metatranscriptomics (Gilbert et al., 2008, Frias-Lopez et al., 2008), metaproteomics (Ram et al., 2005), and metabolomics (Segata et al., 2013), sometimes informed by stable isotope probing (Starr et al., 2018). Although these methods may generate hypotheses about organism interdependencies, our ability to test predicted interdependencies in a community context is extremely limited and largely restricted to highly specialized techniques (Pierce and Dutton 2022).

Microbial community models can infer the sum of all interactions (Skwara et al., 2023, Quinn-Bohmann et al., 2024), but lack of species-resolved mechanistic understanding limits our ability to engineer these systems. Metabolic models can predict interactions by incorporating microbial metabolic capacities (Dukovski et al., 2021), but this approach is primarily limited to co-cultures and simple synthetic communities. This motivates the search for approaches that can elucidate organism-organism interactions in complex microbial ecosystems.

Bacteriophages offer a highly targeted way to probe microbial interactions due to their inherent bacterial specificity and potent host-killing efficiency. Bacteriophages have been predominantly used as therapeutics to remove or deplete pathogenic and antibiotic resistant microorganisms (Buttimer et al., 2022; Thanki et al., 2022; Das et al., 2015, Strathdee et al., 2023; Liao et al., 2025). Bacteriophage can also be further engineered for improved host killing and broadened host range (Selle et al., 2020; Gencay et al., 2023).

Prior work has established that phage hold enormous potential for microbiome manipulation. Carlson et al. (2023) demonstrated that the ammonium-generating capacity of fresh-water enrichments could be altered through the use of applied bacteriophage. Li et al. (2022) demonstrated the depletion of a specific *E. coli* using T7 phage can modulate host phenotypes, specifically animal behaviour. While several studies have engineered phage for increased killing efficiency (Selle et al., 2020), depletion of antibiotic resistance encoding plasmids (Bikard et al., 2014) and modification of host range (Gencay et al., 2023).

Here, we isolated multiple lytic bacteriophages specific to a collection of *Variovorax* isolates, and used them to modulate microbiomes to test several predicted microbial interactions. Our findings demonstrate that phages can be used to probe microbial interactions in the context of complex microbial communities.

Results

Variovorax phage isolation

To isolate *Variovorax* phages capable of selectively killing *Variovorax SCN45* we extracted phage viromes from six rhizosphere and compost samples (Oakland, CA) and tested for infectivity against a panel of *Variovorax* strains (Methods). We isolated nine phages that can replicate in one or more *Variovorax* species. These double-stranded DNA phages ranged in genome size from 43 to 159 Kb and with GC contents of 53% to 66%. Based on protein homology, seven of these phages (all with ~50 kbp genomes) were grouped with other RefSeq phages (Fig. 1a) classified predominantly with *Siphoviridae* (now *Siphovirus*) and share a high degree of average nucleotide diversity (ANI) with each other (Fig. 1b). The remaining two phages clustered with *Myoviridae* and *Autographiviridae* families. Two *Siphoviridae* phages (bapic4 and V.45_iii) and the large *Myoviridae* phage (V.45_v66) showed strong lytic activity against *V.* SCN45 (Fig. 1e). V.45_v66, bapic4 and V.45_iii were shown by TEM to have *Siphovirus*-like morphology, consisting of an icosahedral head and long filamentous tails, similar to the well-known lambda phage (Fig. 1d). All nine of the isolated phages are predicted to be restricted to a lytic lifestyle based on the absence of integrase genes. There was very limited cross-reactivity of the phages between the different *Variovorax* strains (Fig. 1c) based on spot assays. Only one phage, V.45_66, was able to form plaques on multiple hosts - *V.SCN45* and *V. paradoxus DSM 645* (Fig. S1).

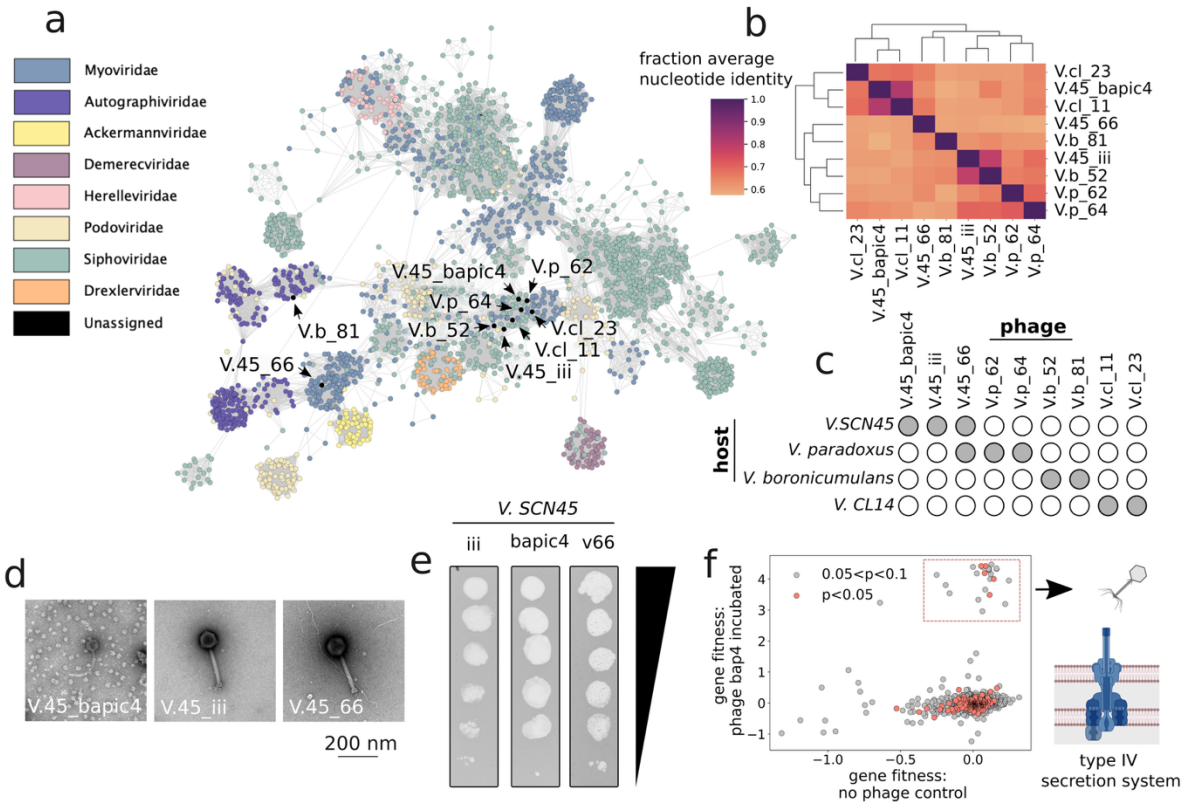

Figure 1. Characterization of nine isolated *Variovorax*-infecting bacteriophages. (a) Protein similarity network of phages deposited in RefSeq and those isolated in this study (black), with edges indicating a significant shared protein content. (b) Pairwise average nucleotide identity (ANI) between the nine isolated *Variovorax* phages. (c) Plaque assays demonstrate limited cross-reactivity of the nine phages across four different *Variovorax* strains, with filled circles representing the ability to plaque on a given host. These include *V.* SCN45, *V.* CL14, *V. boronicumulans* DSM 21722, *V. ginsengisoli* DSM 25185 and *V. paradoxus* DSM 645. (d) Transmission electron microscopy (TEM) of the SCN45-infecting phage, showing icosahedral heads and filamentous tails characteristic of Siphoviridae. (e) High titre phage stocks visualized by 10-fold dilution 1uL spot assays from 10^{-6} to 10^{0}. (f) Genome-wide fitness profiling (RB-TnSeq) for *V. SCN45* genes, following exposure to phage bapic4, identifies the Type IV pilus as the likely receptor used by the phage for infection. Phages V.45_66 and V.45_iii generated similar gene fitness results.

Variovorax SCN45 phages infect via chromosome-encoded type IV pilus

To identify loss-of-function gene disruptions that could confer *Variovorax* with increased fitness under phage infection we constructed an RB-TnSeq mutant library of *Variovorax* SCN45 and employed methods similar to Mutalik et al. (2020). The disruption of genes of the type IV secretion system (T4SS) were found to substantially enhance the fitness of *Variovorax* when incubated with each of its three phages (Fig. 1f). None of these T4SS gene knockouts were enriched in the no-phage controls, indicating that the addition of phage selected for these gene mutants through the elimination of susceptible mutants.

Evaluating Phage-Mediated Depletion in the *Arabidopsis*-*Variovorax*-*Arthrobacter* System

Finkel et al. (2020) demonstrated that *Variovorax CL14* mitigates a root stunting phenotype in *Arabidopsis* by consuming excess auxin secreted by *Arthrobacter* that leads to root stunting. To test whether such well-characterized interactions could be tested through phage-based manipulation, rather than conventional strategies, we hypothesized that a co-culture of the two organisms would result in a normal root phenotype but phage-mediated depletion of *V.* CL14 would result in the accumulation of auxin and cause a stunted root phenotype. We employed a phage cocktail of the Siphoviridae phage V.cl_11 and V.cl_23 to deplete *V.* CL14 from both pure cultures and co-cultures with *Arthrobacter CL28* inoculated onto *Arabidopsis thaliana*. Phage treatment led to the reintroduction of root stunting phenotype (Fig. 2).

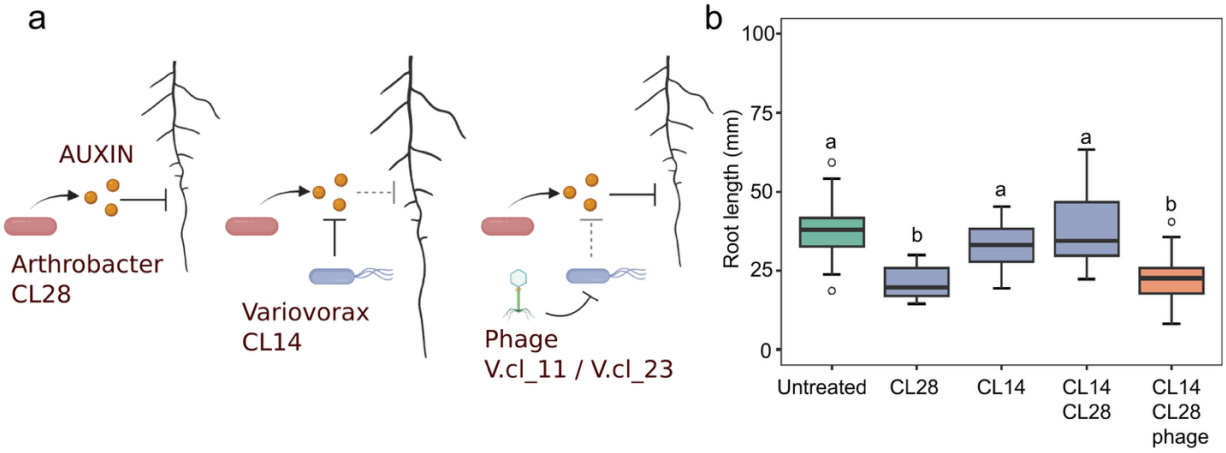

Figure 2. Phage-mediated depletion of *Variovorax* from an *Arabidopsis*-inoculated synthetic community induces root stunting. (a) Model of root inhibition by the auxin-secreting *Arthrobacter* CL28, which reverts to a normal root phenotype when the auxin-degrading *Variovorax* CL14 is present. If the *Variovorax*-targeting phage cocktail (V_11, V_23) is effective in the rhizosphere, this would disrupt the interaction and the root would revert to stunted growth. (b) *Arabidopsis* primary root elongation with *Arthrobacter* CL28 causes a stunted root phenotype, which recovers with *Variovorax* CL14 co-culture. The addition of the *Variovorax*-targeting phage cocktail (V.cl_11, V.cl_23) to the co-culture of *Arthrobacter* CL28 and *Variovorax* CL14 recapitulates the root stunting phenotype observed in the presence of *Arthrobacter* alone. Letters above bars indicate the results of a Tukey post hoc test (α=0.05).

Development of stable enrichment communities

To perform community manipulation experiments it is critical to generate stable, reproducible consortia with reasonable complexity, ideally containing organisms that are predicted to be interdependent on other community members. This study leveraged inoculum from lab-scale bioreactors from which the *Variovorax SCN45* pure culture was previously isolated (Hessler et al., 2023). *Variovorax SCN45* overproduces thiamine in pure culture and was predicted to supply this essential vitamin to highly dependent thiamine auxotrophs in bioreactor communities based on ecological network analyses (Hessler et al., 2023). The thiamine auxotrophs that were

correlated with *Variovorax* had very few correlations with other thiamine-producing organisms, suggesting a strong dependence.

We supplemented additional *Variovorax* SCN45 cells to increase its abundance in inoculum consortia based on previous findings that initial ratios of organisms can affect the final steady state community composition (Gao et al., 2021). The inoculum was then grown in minimal media, supplemented with various carbon sources, and passaged every 48 hours for a total of seven passages (Fig. 3a) and community compositions assessed. Four carbon sources were chosen for ongoing experiments because the communities were reproducible (Fig. 3, S2). The communities included *Leifsonia*, multiple Xanthomondales and several *Microbacterium*, taxa that were predicted to depend on *Variovorax* for thiamine (Hessler et al., 2023).

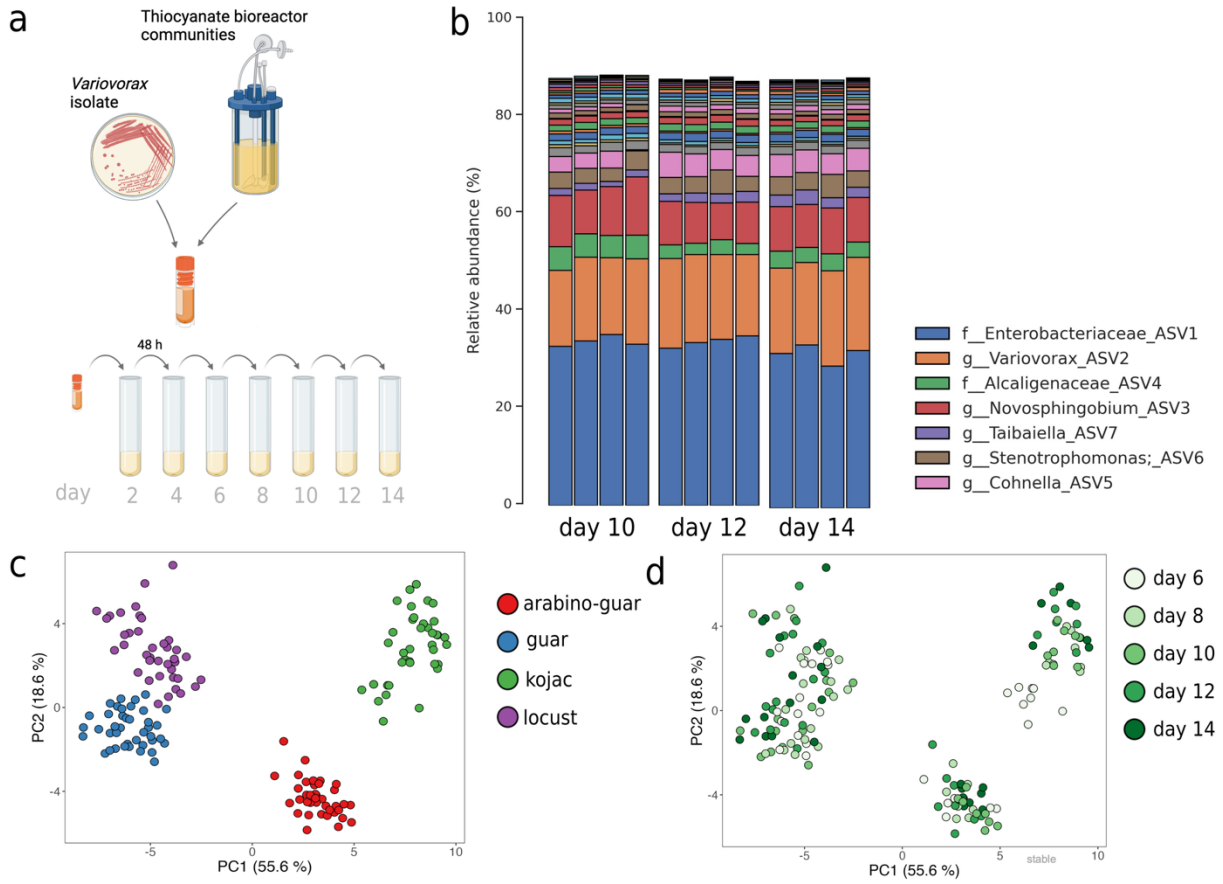

Figure 3. Development of stable enrichment communities. (a) Schematic of Bioreactor-derived inoculum preparation and enrichment passaging. (b) Communities supplemented with guar gum showed reproducible compositions across technical replicates and demonstrated stability across multiple passaging cycles using 16S rRNA gene amplicon sequencing. PCA was performed on robust centered log-ratio (rclr) transformed ASV relative abundances, demonstrating the compositional (c) reproducibility and (d) longitudinal stability were consistent across the cultures supplemented with arabinogalactan with guar gum, guar gum alone, kojac gum, and locust bean gum.

Phage-mediated *Variovorax* depletion leads to broad community impacts

Following the passage of the day 8 communities, either the phage V.45_v66 or a cocktail of three *Variovorax* phages (V.45_v66, V.45_iii, and V.45_bapic4) was added to the communities (Fig. 4 a). The relative abundance of *Variovorax* in the guar gum enrichment was reduced from approximately 22% in the day 8 communities to 2.4% in the day 10 community but further recovered to 11% by day 12 (Fig. 3b). This pattern was consistent across all four communities (Fig. S2). There was minimal difference in the abundance of *Variovorax* between the single phage V.45_v66 and three-phage cocktail, except in the kojac gum- community, where the three-phage cocktail resulted in a lower *Variovorax* abundance (mean 4%) compared to the single V.45_v66 phage (mean 10%) following passage six (day 12).

The overall community structure was impacted by the addition of phages, as evidenced by a notable shift in the principal component two of the PCA (Fig. 4c-e) performed on log-normalized abundance data from amplicon sequencing data. Despite phage addition, community stability was re-established, both in terms of species composition (Fig. 3c-f) and optical density over subsequent passages (Fig. S3). Bacteria other than *Variovorax* that can produce thiamine did not proliferate following *Variovorax* depletion (Fig. 4f). There was no evidence that *Variovorax* phages interacted with non-target organisms that encode a Type IV secretion system (Fig. 4g).

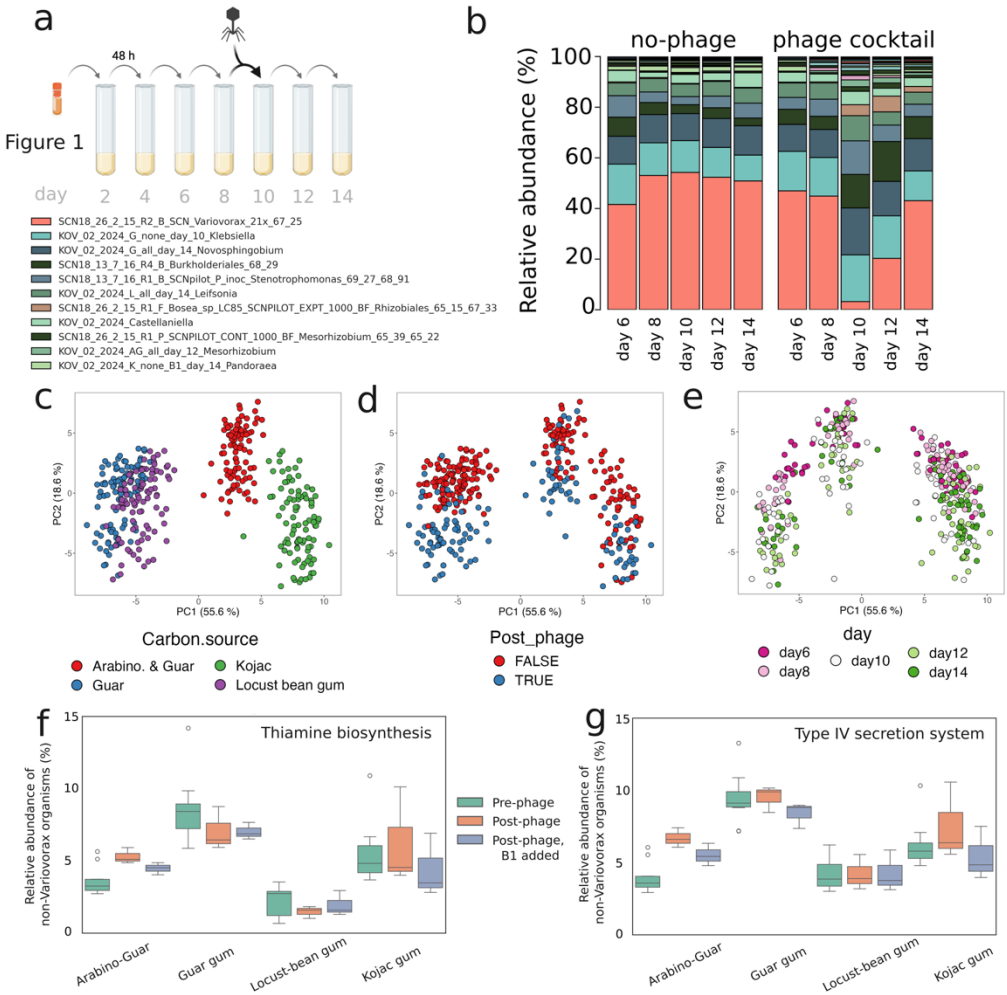

Figure 4. Phage-mediated *Variovorax* depletion across enrichment cultures. (a) Schematic adapted from Figure 3, illustrating the introduction of phage to 2 x10^4 plaque-forming units per mL (PFU/mL) on day 8 following passaging. (b) Genome-resolved metagenomics revealed a marked reduction of *Variovorax* (pink) on day 10 post-phage. Principal component analysis (PCA) of log-normalized abundance data from amplicon sequencing data (c) reveals a separation along PC1 driven by carbon source, while (d) PC2 captures the divergence from pre- and post-phage conditions, and (e) day of the experiment. The summed relative abundance of all organisms encoding (f) a complete thiamine biosynthesis pathway and (g) a type IV secretion system (excluding *Variovorax* from 100% relative abundance). Shown across three stages: pre-phage addition (day 6 and day 8 communities), post-phage addition (day 10, 12, and 14 communities) and post-phage communities supplemented with 10 mg/L thiamine (B1).

Variovorax depletion confirms dependence of specific thiamine auxotrophs

We assessed which organisms exhibited statistically significant abundance changes between the 'pre-phage communities' (day six and day eight communities) and the communities following the addition of phage (day 10, 12, 14 communities). After phage administration, we added thiamine to the control enrichment communities to identify the organisms that were specifically reliant on *Variovorax* for thiamine. Amplicon sequencing of the four enrichment cultures revealed that some

203 organisms that decreased in abundance following *Variovorax* depletion, and then increased
204 significantly in abundance following thiamine supplementation (Fig. 5a). These included a
205 *Lysobacter* (Xanthomonadales*)*, a *Leifsonia,* and microorganisms belonging to the family of
206 Microbacteriaceae (Fig. 5b). Genome-resolved metagenomics of the samples revealed that the
207 *Leifsonia* (Fig. S5), a *Microbacterium* and a *Stenotrophomonas* (Xanthomonadales) all lack a
208 complete thiamine biosynthesis pathway (Supplementary data).
209
210 To determine if the association between *Leifsonia* species and thiamine-producing bacteria may
211 be more general, we assessed 32 *Leifsonia* genomes present in GTDB for the ability to synthesize
212 thiamine. We found only a single *Leifsonia* genome to have a complete pathway (Supplementary
213 data).
214
215
216
217
218
219

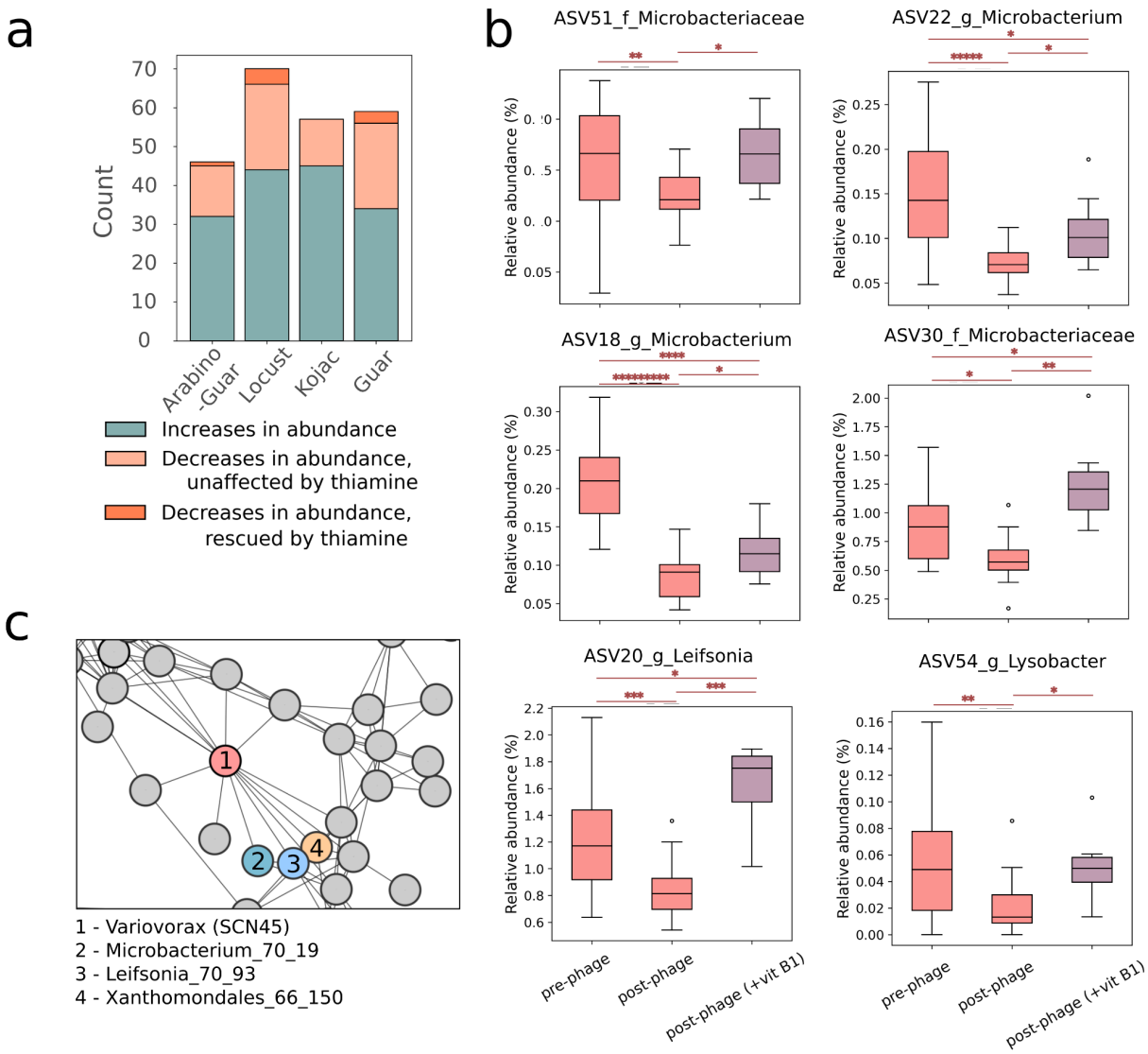

Figure 5. Previously identified organisms experimentally confirmed to rely on *Variovorax* for thiamine. (a) Amplicon sequence variants (ASVs) exhibiting significant changes in relative abundance between the pre- and post phage communities. Many ASVs increased in abundance following *Variovorax* depletion while others showed reduced abundance, and with a subset of these demonstrating recovery following the addition of thiamine. (b) Six ASVs corresponding to multiple *Microbacteria*, a *Leifsonia*, and a *Lysobacter* show a reduced abundance following the depletion of *Variovorax* but returned to near original levels with the supplementation of thiamine. (c) Closely related strains of these organisms appear in the correlation network that was initially used to predict *Variovorax* as a thiamine-producer and show correlations with *Variovorax* (Hessler et al., 2023).

SNPs enabled post-infection recovery of *Variovorax*

The *Variovorax* SCN45 genome is comprised of a 6.8 Mb chromosome and 1.2 Mb circular genetic element that is related to a *Variovorax paradoxus S110* sequence described as a “second chromosome” by Han et al. (2010). *Variovorax* SCN45 lacks CRISPR-Cas systems but encodes

24 PADLOC(v4.3.0)-predicted phage defence systems. We were unable to detect any deletions of these genes, or of any genes (including those of the T4SS), in post-phage *Variovorax* populations based on read mapping and gene abundances.

To seek evidence for mutations that could confer phage immunity in surviving *Variovorax* populations, we monitored *Variovorax* single-nucleotide polymorphisms (SNPs) across the four experiments. Before the introduction of phage, the majority of reads map to the reference genome without SNPs. However, following phage addition, there is a marked increase in the representation of SNPs and an increase in the number of SNP sites. In prephage communities the majority of wildtype haplotypes are present at approximately 90% (indicating that at a given SNP site, 90% of mapped reads support the wildtype base). However, following phage infection the proportion of SNP sites with the wildtype haplotype reduces, demonstrating selection of new or previously less abundant SNPs (Fig. 6a, S6).

Although most SNPs post-phage infection were synonymous, a subset was not. To identify new gene variants under strong selection, we identified regions of the genome with SNPs that were closely spaced enough that linkage could be established. Some regions with high densities of linked SNPs occurred in both the no-phage controls and post-phage populations (Fig. 6b) and thus were likely beneficial under all conditions (Fig. 6c). These included genes related to aerobic benzoyl-CoA catabolism, a type V secretion system, enoyl-CoA hydratase, and cell envelope structural proteins. However, there was a single region of the *Variovorax* genome that showed high SNP linkage density only in the post-phage populations. This locus encoded multiple conjugal transfer proteins (Fig. 6c). Most importantly, we identified two non-synonymous SNPs in the *trbE* conjugal transfer protein (homologous to *virB4*) within the P-loop domain which alters the charge and hydrophobicity of this region of the protein.

To identify SNPs that were not close enough to other mutations to provide linkage, we recovered all non-synonymous SNPs that increased in abundance by at least 30% in the post-phage populations relative to the pre-phage and no-phage control populations. We identified 275 gene variants found exclusively in post-phage populations (Supplementary data). Several were associated with known phage defence systems including the retron XIII, Lamassu family, and putative PDC-S02 defence systems. Most interesting were three SNPs detected in three or more of the four communities. This group of genes included a filamentous haemagglutinin family outer membrane protein, a redoxin/thioredoxin-like sensor protein associated with a fatty acid biosynthesis operon, and a protein with domain of unknown function (DUF932). This DUF932 gene occurs within an integrated plasmid that encodes *parA*, *parB*, an integrase, a plasmid transfer protein (*tral*), and a replication initiation protein (*repA*). Notably, multiple non-synonymous SNPs occurred in the DUF932 protein, and these variants were exceptionally abundant, exceeding 70% in the post-phage populations. In contrast, the *trbE* gene displayed non-synonymous SNPs in 21-33% of reads from post-phage populations. Interestingly, the start codon of this DUF932 gene was mutated to AAG (lysine) in 50-60% of each of the four populations. This likely impacts translation initiation and results in truncation of the protein as the next in-frame AUG codon occurs in position 66.

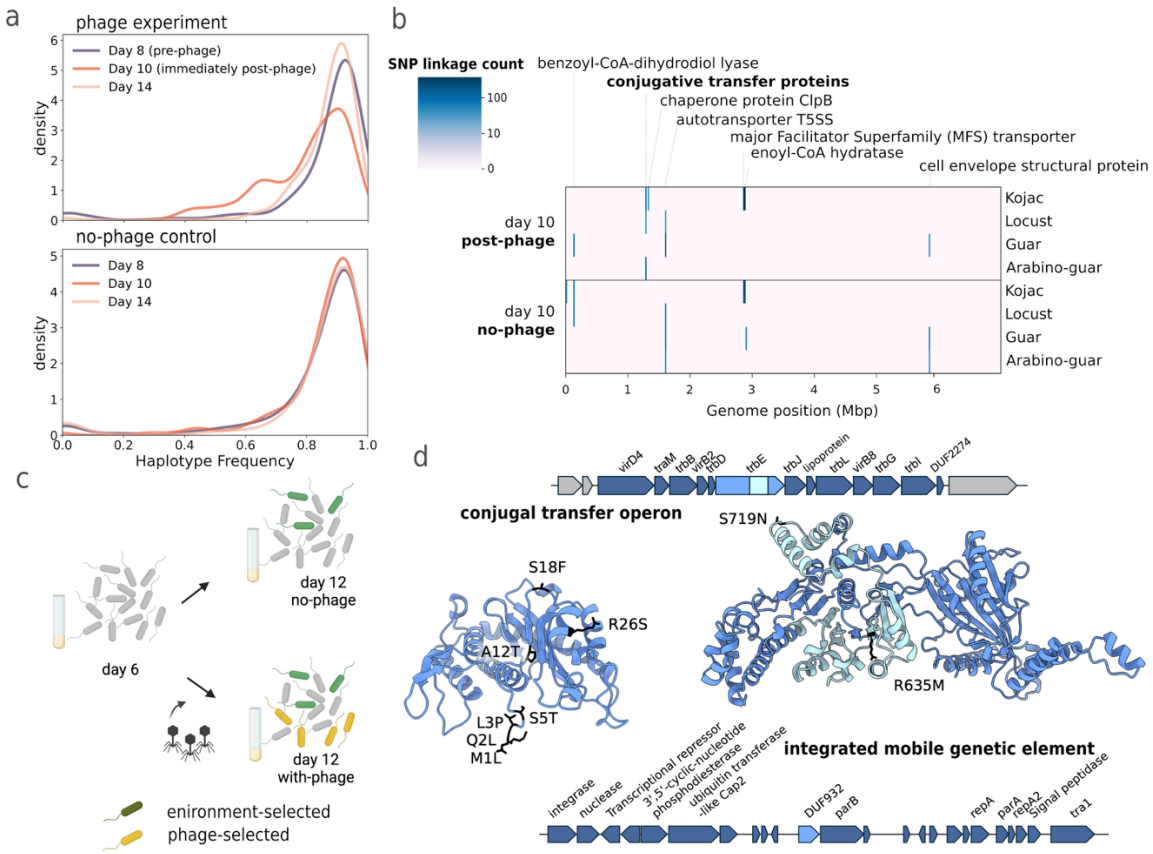

Figure 6. Phage infection induces shifts in *Variovorax* populations and selects for consistent gene variants. (a) Haplotype frequency distributions of *Variovorax* populations in the locust bean gum communities shows the impact by phage application, with expansion of low abundance SNPs, followed by return to pre-phage distributions. (b) Post-phage *Variovorax* populations show increased linked-SNP density in a conjugative transfer gene operon, visualised by a heatmap. Linked-SNPs associated with three 16S rRNA genes have been removed for clarity. (c) A schematic illustrating different categories for selection in day 12 communities. (d) Gene operons and AlphaFold-predicted protein structures showing consistent mutation sites within the conjugal transfer protein TrbE and domain of unknown function within an integrated genetic element.

Variovorax relies on its own thiamine biosynthesis in all enrichment cultures

To investigate genes important for *Variovorax* fitness in enrichment cultures (in the absence of phage), we introduced the *Variovorax* SCN45 RB-TnSeq mutant library into each of the four enrichment cultures (Fig. 7a). In all four of the communities, knockouts of multiple genes involved in the biosynthesis thiamine (*thiC*, *thiG*, *thiE, purE* and *purK)* had a strong negative fitness impact on *Variovorax* (See Fig. S6 for an overview of the pathway). These results indicate that in the four enrichments, *Variovorax* was reliant on its own biosynthesis for thiamine and little extracellular thiamine was likely available.

Rate of recovery of *Variovorax* populations correlates with reduced dependence on Type IV secretion system

Phage treatment reduced the abundance of *Variovorax* to approximately 3% in all day 10 post-phage communities, but *Variovorax* showed the fastest recovery in the guar and locust-bean gum communities over the following days (Fig. 7b). The *Variovorax* populations in these two communities (Fig. 7c, S5) had SNP concentrations close to pre-phage levels by day 14.

We amended enrichments with the RB-TnSeq mutant library to investigate the consequences of specific gene knockouts for *Variovorax* fitness in the four communities (in the absence of phages; Fig. 7a). In the guar and locust-bean gum communities the knockout of the T4SS was advantageous, based on selection for these genotypes. In contrast, these knockouts were mildly deleterious in the arabino-guar and kojac gum substrate-amended communities.

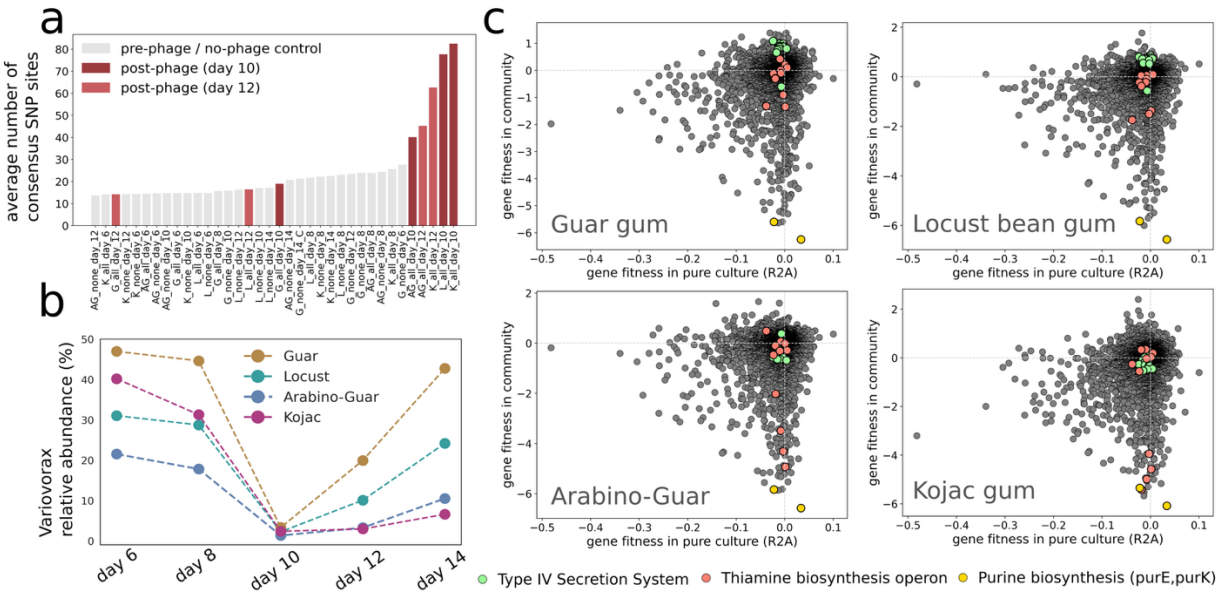

Figure 7. The rate recovery of *Variovorax* populations from phage infection corresponds to the fitness conferred by the type IV secretion system (T4SS). (a) Genome-wide fitness profiling (RB-TnSeq) for *V. SCN45* showing the fitness of gene-knockouts in each of the four communities (y-axis) versus in pure culture in R2A, rich media (x-axis), highlighting the type IV secretion system and thiamine biosynthesis genes. (b) Relative abundance of *Variovorax* is reduced to ~3% in all post-phage communities, with a gradual recovery over the following passages, again fastest in the guar and locust bean gum communities. (c) Genome-wide SNP sites in *Variovorax* populations increase immediately following phage infection (day 10) but decline to pre-phage levels, with the guar and locust bean gum populations recovering the fastest. Read mapping was normalized to 20x coverage for all *Variovorax* populations.

Discussion

Previously, networks constructed using organism abundance data allowed us to identify thiamine auxotrophs that were strongly correlated with *Variovorax* (SCN45) in the bioreactor communities

324 studied here (Hessler et al., 2023). Subsequently, we showed that *Variovorax* produces high
325 concentrations of extracellular thiamine in pure culture, however we did not verify that this
326 thiamine production was sustained within natural communities. To better explore possible
327 interdependence related to vitamin provision required experiments conducted in communities
328 from which *Variovorax* could be selectively removed, without directly impacting the rest of the
329 community. We hypothesized that highly targeted community manipulation could be achieved via
330 use of *Variovorax*-specific phages.
331
332 To demonstrate the feasibility of testing organism-organism interactions using phage-mediated
333 *Variovorax* depletion, we leveraged the *Arabidopsis*-*Variovorax* CL14-*Arthrobacter* system first
334 characterized by Finkel et al. (2020) in which *V. CL14* mitigates root stunting in *Arabidopsis* by
335 degrading auxin produced by *Arthrobacter*. Following the addition of isolated phages V.cl_11 and
336 V.cl_23 to this co-culture, we observed a pronounced root-stunting phenotype, indicating that the
337 phages successfully depleted *Variovorax* CL14 (Fig. 2). These findings highlight the potential of
338 extending phage-mediated testing of microbe-microbe and microorganism-plant interactions to
339 rhizosphere microbiome manipulations for agricultural applications.
340
341 Next, we used three isolated *Variovorax* SCN45 phages to selectively deplete this *Variovorax*
342 from four enrichment communities and monitored the effects on the remaining community (Fig. 4,
343 5). The subsequent addition of thiamine facilitated the recovery of only a *Leifsonia*, a
344 Xanthomondales, and a *Microbacterium*, each lacking complete thiamine biosynthesis pathway.
345 This provides clear evidence that *Variovorax*-produced thiamine was supporting the growth of
346 these specific organisms in the communities and demonstrates the effectiveness of phage-
347 mediated knock-down experiments for capturing these metabolic interactions. Related, but non-
348 identical, strains of *Leifsonia*, *Microbacterium,* and the Xanthomondales were among a larger
349 group of organisms associated with *Variovorax* in the correlation network from which the thiamine-
350 exchange hypothesis was developed (Hessler et al., 2023).
351
352 Using a *Variovorax* SCN45 RB-TnSeq mutant library we found that disruptions in the *Variovorax*
353 type IV secretion system genes conferred phage immunity, indicating that the three phages tested
354 all infect via this complex. The T4SS is a common target for phage attachment and genome
355 injection (Russell 1995; Berry et al., 2011). One potential concern is that depletion of *Variovorax*
356 might occur following phage infection, yet decreased abundance of correlated organisms could
357 be due to toxicity following uptake of viral DNA via T4SSs. Countering this, we find that encoding
358 of a type IV secretion system was not a predictor of whether an organism decreased in abundance
359 following phage addition. Thus, we concluded that these phages could be used to directly identify
360 the organisms that are dependent on *Variovorax* SCN45 in the bioreactor consortia and the basis
361 of the dependence.
362
363 *Variovorax* populations demonstrated partial to complete recovery from phage infection by the
364 end of the experiment. We were unable to identify any gene deletions, frameshift mutations or
365 non-synonymous SNPs in T4SS genes. However, by investigating genes with enriched non-
366 synonymous SNPs, we identified gene variants of the *TrbE* conjugal transfer protein in *Variovorax*
367 that arose following phage treatment. TrbE physically interacts with the T4SS and is a member of

368 the *VirB4* family of proteins responsible for substrate recruitment and transfer to the secretion
369 channel of T4SS (Li et al., 2018; Redzej et al., 2022). We observed two non-synonymous SNPs
370 within the P-loop domain of this protein which is responsible for ATP binding and hydrolysis. We
371 speculate that the *trbE* mutations interfere with the functioning of the T4SS required for phage
372 infection.
373
374 In addition to *trbE* variants, we observed non-synonymous SNPs in a small-protein-coding
375 (DUF932) gene within a putative integrated plasmid in all phage-treated *Variovorax* populations.
376 Although the precise role of this gene is unclear, its consistent selection after phage application
377 strongly suggests involvement in phage defence. The blocking of phage entry by resident mobile
378 genetic elements, including phage, is well-documented (Kliem & Dreiseikelmann, 1989; Berry and
379 Christie, 2011; Kamruzzaman et al., 2022; Johnson et al., 2022; Taylor et al., 2024; Rivard et al.,
380 2024;). For example, the *pVII* minor capsid protein in *Pseudomonas* phage *Pf4*, interacts directly
381 with the host *PilC* protein, responsible for T4SS assembly in *Pseudomonas*, rendering it inactive
382 and preventing phage superinfection (Wang et al., 2022). We suspect that *Variovorax* developed
383 phage resistance through both chromosomal and mobile element-mediated modulation of the
384 T4SS. These mutations are likely to have existed within the *Variovorax* populations prior to phage
385 application and highlight the role of population variation in surviving phage infection.
386
387 The addition of a single or multiple phages showed little difference in *Variovorax* depletion or its
388 rate of recovery. This absence of additive effects has been observed in other studies (Pyenson
389 et al. 2024), including efforts to remove *Ralstonia* from tomato plants (Franco Ortega et al., 2024).
390 In our study, this may have occurred to all three *Variovorax*-targeting phages infecting via the
391 same receptor. In future studies, the use of multiple phages targeting different receptors would
392 likely be beneficial, as has been shown in phage-therapy research treating bacterial infections in
393 humans (Yoo et al., 2024). However, complete bacterial removal is rare and, in clinical cases, has
394 required the simultaneous use of antibiotics (Pirnay et al., 2024). Notably, in the *Ralstonia*-
395 infected tomato plant studied by Wang et al. (2019), the addition of phages resulted in the
396 enrichment of taxa that naturally suppressed the growth of *Ralstonia* through antibiotic production.
397 These studies suggest that phage application alone is unlikely to remove target bacterium long-
398 term, and that additional ecological or therapeutic pressures are required to sustain suppression
399 of the target organism. However, as we show here, even partial and temporary depletion of
400 populations is useful to test interaction hypotheses.
401
402 *Variovorax* recovered at variable rates following phage treatment, with communities in which
403 T4SS knockouts conferred positive fitness exhibiting the fastest recovery. Prior work has shown
404 that community composition can substantially impact phage-host dynamics (Blazanin and Turner,
405 2021; Alseth et al. 2019). Phage susceptibility can also be strongly influenced by the natural
406 variation in physiology of genetically identical cells, such as cell size (Schenk & Sieber, 2019) and
407 receptor protein copy numbers (Chapman-McQuiston & Wu, 2008; Igler et al., 2022). This leads
408 us to hypothesize that community- and environmental selection against T4SS expression in
409 *Variovorax* in the guar and locust bean gum communities could have led to reduced presentation
410 of this complex by *Variovorax*, thereby limiting infection by our phages targeting this system. The
411 observed variation in *Variovorax* recovery highlights how community context could impact phage

infection, and may be an important area of research for the application of phage-based microbiome manipulations.

Here, we establish the basis of specific microbe-microbe interactions in natural enrichment-based communities by isolating and using phages to selectively deplete a member of interest. This approach addresses a critical challenge in microbial ecology by easily enabling the direct testing of interaction hypotheses within natural consortia, including interactions involving taxa that are otherwise difficult to culture or manipulate. This method is scalable, cost-effective and uses standard microbiology techniques without requiring specialized equipment. Although suitable phage isolation does require the isolation of the microorganism of interest, future integration of phage engineering with advances in protein design (Pacesa et al., 2025) may circumvent this current limitation. Overall, phage-based approaches represent valuable tools for understanding the structure of microbial communities and offer promising avenues for microbiome engineering.

Methodology

Bacterial inoculum preparation

Variovorax was grown overnight from a single colony in R2A media. 100 mLof planktonic phase cells were recovered from two bench-scale thiocyanate-degrading bioreactor systems, from which *Variovorax* was initially isolated a year prior. Flocculated particles were allowed to settle to the bottom of the container for 30 min and the top 50 mLwere carefully removed. 10 mLof bioreactor planktonic phase were added into 50 mLfalcon tubes. 5 mLof *Variovorax* overnight culture was added to this falcon tube. 15 mLof 50% glycerol was then added and mixed by swirling and inverting each tube. 200 uL of each culture were distributed into cryo tubes, frozen in liquid nitrogen, and stored at -80C. This approach was based on previous inoculum ratio testing experiments (Gao et al., 2021), which demonstrated that a higher abundance of a member in the inoculum improves its chances of establishing within the community.

Community passaging

Inoculum glycerol stocks were thawed on ice and gently mixed by pipetting. 50 uL of glycerol stock was added to 10 mLof M9 minimal media in quadruplicate supplemented with 50 ug/L cycloheximide, 10 mg/L pantothenic acid, and a trace metal solution described by Watts et al. (2019). Culturing was performed using four independent technical replicates to provide robustness for statistical tests. The electron donors used were 0.2 g/L of kojac gum, locust bean gum, guar gum, and combined 0.1 g/L guar gum and 0.1 g/L arabinogalactan. Under each electron donor condition, following inoculation, cultures were incubated at 30C for 48 hours with shaking at 140 rpm. Cultures were passaged using 200 uL of spent medium into 10 mLof fresh media. This was repeated every 48 hours for a total of seven passages over 14 days. This culturing protocol was heavily informed by Goldford et al. (2018). The glycerol stocks were then used to inoculate fresh tubes followed by two passages as described above. At each passage step, 8 mLof culture were centrifuged at 10,000 X g for 10 minutes and cell pellets were frozen at

450 -80C for subsequent DNA extraction. 200 uL of spent medium was used to perform OD
451 measurements using a 96-well plate reader at 600 nm.

452 Virome preparations

453 Three sources of viromes were collected: (i) soils, (ii) composts and (iii) and thiocyanate-
454 degrading bioreactors. Briefly, approximately 10 grams of soil or compost were collected in falcon
455 tubes and incubated with 25 mLof SM buffer with shaking for one hour. In the case of bioreactor
456 viromes, biofilm material was removed from the bioreactors using serological pipettes and
457 subjected to metal bead beating on a vortex at maximum speed for ten minutes to disrupt the
458 biofilm. For all three types of viromes, the particulate matter was then allowed to settle for 30
459 minutes before the supernatant was removed and centrifuged at 10,000 X g for 10 minutes and
460 the supernatant then passed through a 0.22 um filter.

461 Phage liquid enrichment

462 Bacteria were grown overnight from single colonies in 10 mLof R2A media and incubated at 30C
463 at 160 rpm. Cultures were back diluted into fresh R2A containing 2 mM MgCl2 and 2 mM CaCl2
464 to an OD600 of 0.03-0.05. Cultures were allowed to grow until reaching an OD600 of 0.15-0.3.
465 Subsequently, 100 uL of viromes were then added to the tubes and the cultures were incubated
466 for a further 24 hours. The cultures were then sampled and cells were removed by centrifugation
467 at 10,000 X g for 10 minutes. This supernatant served as the virome for the next round of
468 enrichment. This process was repeated for a total of five enrichments.

469 Phage isolation: Plaque assays

470 Plaque assays were performed on the *Variovorax* strains *V.* SCN45, *V.* CL14, *V. boronicumulans*
471 (DSM 21722), *V. ginsengisoli* DSM 25185 and *V. paradoxus* DSM 645. These strains were grown
472 overnight from single colonies in 10 mLof R2A media and incubated at 30C at 160 rpm. Cultures
473 were back diluted into fresh R2A to an OD600 of 0.03-0.05. Cultures were allowed to grow until
474 reaching an OD600 of 0.15 - 0.3. Subsequently, 100uL of log-phase cells were added to 20 uL of
475 0.2 um filter-sterilized viromes and incubated at RT for 10 minutes. These were mixed with 50C
476 R2A (2 mM MgCl2 and 2 mM CaCl2) 0.5% top agar and plated onto R2A 1.5% bottom agar plates.
477 Plates were incubated at 30C for 48 hours and inspected for plaques. Plaques were picked using
478 sterile 100 uL tips into 100 uL of SM buffer.

479 Phage genome sequencing, assembly and annotation

480 DNA from phage suspensions were extracted using Zymo Quick-DNA viral kits using
481 manufacturers instructions. Extracted DNA was then Illumina shotgun sequenced on a Novaseq
482 using 150PE reads with a 300 bp insert size and yielding 1 Gbp per sample. Viral genomes were
483 assembled using Metaviral-Spades (Antipov et al., 2020) and extended using COBRA (Chen et
484 al., 2024). The genomes were then annotated using vogDB (Trgovec-Greif et al., 2024), Pfam
485 (Bateman et al., 2004) and KEGG (Kanehisa & Goto, 2000) hidden Markov models using
486 hmmscan. Protein sharing of the nine phage and Refseq and was performed using Vcontact2

487 (Bin-Jang et al., 2019). Phage genome ANI was determined using Vclust (Zielezinski et al., 2024;
488 https://github.com/refresh-bio/vclust).

489 Transmission electron microscopy (TEM)

490 Virus particles were visualized using a FEI Tecnai T12 Transmission Electron Microscope at an
491 accelerating voltage of 80 kV. Carbon-coated copper grids were charged in a vacuum chamber
492 followed by application of 5 uL of virus suspension and allowed to dry. The grids were washed
493 with deionised water three times before negative staining in 1.0 % ammonium acetate for 60s.
494 Grids were allowed to air dry before being visualized.
495

496 *Arabidopsis* inoculation and co-cultures with *Variovorax* CL14, *Arthrobacter* 497 CL28, and V.cl_11+V.cl_23 phage for root length phenotyping

498 *Arabidopsis thaliana* Col-0 seeds were surface-sterilized in 50% bleach for 20 min with 0.05%
499 Tween 20 for 20 min, removing all bleach and rinsing five times in sterile water. Sterile seeds
500 were stratified in the dark for 2 to 3 days at 4°C. A nylon mesh filter with 100 micron pore size
501 was cut to fit on the 100 mm x 100 mm square petri dish as previously described (Cole et al.
502 2017). After stratification, ~7 seeds were placed on the mesh filter on 1.0MS, 0.5% sucrose, 0.6%
503 phytagel plates and grown under long day conditions for 7d (16-h light/8-h dark regime at 22-°C).
504 Bacteria strains preparation: *Variovorax* CL14 and the root growth inhibiting strain *Arthrobacter*
505 CL28 were streaked on agar plates from glycerol stocks, a single colony was transferred to 3 mL
506 liquid R2A media and grown overnight. Cultures were gently pelleted then washed twice with 10
507 mM MgCl2, normalizing the volume of each culture to OD600 = 1, then adjust to OD600=0.04
508 before spreading 50 µl on each plate (Full MS, 0.6% phytagel without sucrose. Full MS was used
509 instead of 1/2X as previously described to maintain the required Mg and Ca concentrations for
510 optimal phage lysis (2mM)). To prepare the phage inoculation, 5 ul of a phage cocktail
511 (Siphoviridae phage V.cl_11+V.cl_23; $1x10^4$ PFU/uL each) was diluted in 500 uL 20 mM MgCl2
512 and 100 ul of this solution was spread onto each plate. After the plants grew 7d, the mesh was
513 transferred to each of the bacteria and phage inoculated plates and returned to the growth
514 chamber vertically grown in short day conditions (16-h dark/8-h light regime at 22°C). Plates were
515 imaged 10 days after transfer. Primary root length was measured using ImageJ software, first
516 setting the scale to the grid on the plate (13 mm) before measuring primary root elongation for
517 each plant. There were three replicate plates (containing n≥5 plants each) for each control and
518 treatment: uninoculated, no bacteria + V11/V23 phage, *Variovorax* CL14, *Arthrobacter* CL28,
519 *Variovorax* CL14 + *Arthrobacter* CL28, *Variovorax* CL14 + *Arthrobacter* CL28 + V11/V23 phage.

520 Phage-perturbed community experiments

521 Stable communities were grown on selected carbon sources and exposed to *Variovorax*-specific
522 phages (V45_v66, or a three-phage cocktail of V45_v66, V.45_iii, and V.45_bapic4) 8 hours after
523 the passaging of the day 8 communities (ie. following passage 5), using 50 uL of 4×10^4 PFU/uL
524 each per 10 mLculture. Experiments were conducted in quadruplicate with a no-phage control

525 included for comparison. The final varied condition involved the presence or absence of 10 mg/L
526 thiamine, administered at the time of phage addition and maintained during subsequent
527 passages.

528 DNA extraction, amplicon and shotgun sequencing

529 Genomic DNA was extracted from cell pellets using the Qiagen DNeasy PowerSoil Pro Kit
530 according to the manufacturer's instructions. V4-V5 16S rRNA gene amplicons were generated
531 by PCR using primers 515F (GTGNCAGCMGCCGCGGTAA) and 926R
532 (CCGYCAATTYMTTTRAGTTT) and cycling conditions 95C 10 min, 72C 90s, 50C 60s, 72C 90s
533 for 30 cycles and a final extension at 72C for 10 min. PCR products were cleaned using Ampure
534 XP magnetic beads. PCR products were sequenced by Innovative Genomic Institute's Next
535 Generation Sequencing Core on an Illumina MiSeq instrument using a read length of 2 x 150 bp
536 with approximately 50,000 reads per sample. Generated amplicon sequencing data was
537 processed yielding ASVs as performed by Kust et al. (2023). Whole genome community library
538 preparation and shotgun sequencing was performed by Novogene. Paired-end Illumina libraries
539 were prepared from genomic DNA with an insert size of 350 bp and sequenced on an Illumina
540 Novaseq producing approximately 6 Gbp of raw sequencing data per sample. The *Variovorax*
541 isolate was subsequently sequenced using PacBio long-read sequencing at 60x coverage, to
542 generate two circular chromosomes.
543

544 Metagenomic Read Processing, Assembly and binning

545 Illumina 150 PE reads from community shotgun sequencing were processed as documented in
546 the ggKbase data preparation pipeline (https://ggkbase-help.berkeley.edu/overview/data-
547 preparation-metagenome/). Reads were processed using BBtools (Bushnell 2020) and sickle
548 (Joshi and Fass, 2011), and were then assembled using IDBA-UD (Peng et al., 2012). Open
549 reading frames (ORFs) were predicted using Prodigal V2.6.3 (Hyatt et al., 2010). Contigs were
550 binned using CONCOCT (Alneberg et al., 2013), Maxbin2 (Wu et al., 2016), MetaBat2 (Kang et
551 al., 2019), and VAMB (Nissen et al., 2021). The best bins per sampled were selected using DAS
552 tools (Sieber et al., 2018) and a final non-redundant genome set across all enrichment
553 communities and the previously published thiocyanate bioreactor genome set found at
554 https://ggkbase.berkeley.edu/SCN_92/organisms was selected using dRep (Olm et al., 2017) at
555 95% ANI.

556 Microbial genome annotation, classification and strain analysis

557 Microbial genomes were then annotated using hmmscan against Pfam (Bateman et al., 2004)
558 and KEGG (Kanehisa & Goto, 2000) databases and were taxonomically classified using GTDB-
559 tk (Chaumeil et al., 2020). All read mappings were performed with bowtie2 (Langmead et al.,
560 2012). Genome coverage and relative abundance across samples were determined using coverm
561 (Aroney et al., 2025). Genome-genome correlation was determined using Fastspar (Watts et al.,
562 2019) which implements the Sparcc algorithm (Friedman et al., 2012). *Variovorax* strain analysis
563 was performed using inStrain (Olm et al., 2021) and the PacBio assembled *Variovorax* genome.
564 Phage defence systems were predicted in the *Variovorax* genome using padlock (Payne et al.,

565 2022, https://padloc.otago.ac.nz/padloc/). Protein structure predictions were performed using
566 Alphafold3 (Abramson et al., 2024. https://alphafoldserver.com/)

567 Statistical analyses

568 Distributions in organism abundances were compared by two-sample t-test assuming unequal
569 variance was performed using the ttest_ind function of the scipy.stats Python package. The
570 abundance of ASVs was calculated excluding the abundance of *Variovorax* contributing to 100%
571 abundance. Relative abundance data were normalized by robust centered log-ratio (rclr)
572 transformation using the decostand function from the vegan R package (Oksanen et al., 2001).
573 Principal component analysis (PCA) was performed on the normalized abundance data using the
574 prcomp function in R to visualize variation in community composition across samples.

575 RB-TnSeq library construction

576 A DNA-barcoded *mariner* transposon mutant library of *Variovorax* SCN45 was generated as
577 described previously (Wetmore et al., 2015; Thorgersen et al., 2021). Briefly, an *E. coli* strain
578 (WM3064) carrying the transposon vector library pHLL250 was conjugated with wild-type
579 *Variovorax* SCN45 at a 1:1 ratio on LB agar plates supplemented with diaminopimelic acid (300
580 uM) for 6 hours. Post conjugation, the transformants were plated onto R2A agar plates containing
581 50 µg/ml kanamycin. Several thousand *Variovorax* colonies were scraped and collected into a
582 tube before being resuspended in 100 mL of R2A with Kanamycin and incubated at 30 C for 6
583 hours. Glycerol stocks (15%) were made and stored at -80C. Cells from the final mutant library
584 were pelleted through centrifugation and their DNA extracted and sequenced by TnSeq-like
585 Illumina sequencing protocol.

586 RB-TnSeq library incubations

587 A 2 mLmutant library glycerol stock was thawed and inoculated into 25 mLof R2A with 50 ug/ml
588 kanamycin and incubated at 30°C with shaking until cells entered mid log phage (approximately
589 8 hours). Four tubes of 2 mLof culture, termed time zero controls, were then recovered and cells
590 pelleted by centrifugation and frozen at -80°C. The remaining cultured cells were then washed
591 twice in relevant media (M9 media without carbon source or R2A) with spins at 3000g for 3
592 minutes. The cells were resuspended in media and inoculated into relevant or culture to a final
593 OD600 of 0.02. The cultures were grown in 10ml glass tubes and incubated at 30 °C with shaking.
594 (i) For phage-challenge experiments 10 uL of phage (4×10^4 PFU/ul) were added to the libraries
595 after 4 hours of subsequent incubation and allowed to incubate for a total of 24 h. (ii) For
596 community incubations, cultures were passaged every 48 h for four passages. Cells were
597 recovered from four replicate cultures by centrifugation and stored at -80 °C. Genomic DNA was
598 then extracted from the stored cell pellets and PCR and sequencing by BarSeq performed as
599 described previously (Wetmore et al., 2015).
600

601 Data availability

602

The contigs representing the *Variovorax* genome assembled by PacBio can be found under bioproject PRJNA1212206 genome accessions CP179718-CP179720. The assembled genomes of the isolated phage have been deposited in GenBank under accession numbers PV558788 - PV558796. The reads associated with these genomes and assemblies can be found under accession numbers SRR33449703 - SRR33449695. The 16S rRNA amplicon sequencing data can be found under Bioproject PRJNA1254325, under accession numbers SRR33264975 - SRR33264785. Shotgun sequencing can be found under bioproject PRJNA1254232, including reads (SRR33436150-SRR33436076), assemblies (SAMN48138949 - SAMN48139025), and novel MAGs (SAMN48122594 - SAMN48122609). These MAGs can also be found on ggkbase https://ggkbase.berkeley.edu/Phage_treated_Variovorax_enrichments_dereplicated_MAGs/ and MAGs detected in this study that had been previously published can be found on ggkbase https://ggkbase.berkeley.edu/SCN_92/.

Acknowledgments

This material by m-CAFEs Microbial Community Analysis and Functional Evaluation in Soils, (m-CAFEs@lbl.gov) a Science Focus Area led by Lawrence Berkeley National Laboratory is based upon work supported by the U.S. Department of Energy, Office of Science, Office of Biological and Environmental Research under contract number DE-AC02-05CH11231. Thank you to the staff at the UC Berkeley Electron Microscope Laboratory for advice and assistance in electron microscopy sample preparation and data collection. We thank Jennifer M. Doudna for institutional support and supervision. Thanks to Leylen Miloslavich, Marta Ortega and Kaitlin Creamer for assistance with lab operations, Henrik V. Scheller and Benjamin J Cole for *Arabidopsis* seeds, and to Jeffery L. Dangl for the *Variovorax CL14* strain and Rebecca S Bart for the *Arthrobacter CL28* isolates.

References

Alneberg, Johannes, Brynjar Smári Bjarnason, Ino de Bruijn, Melanie Schirmer, Joshua Quick, Umer Z. Ijaz, Nicholas J. Loman, Anders F. Andersson, and Christopher Quince. "CONCOCT: clustering contigs on coverage and composition." *arXiv preprint arXiv:1312.4038* (2013).

Alseth, E. O., Pursey, E., Luján, A. M., McLeod, I., Rollie, C., & Westra, E. R. (2019). Bacterial biodiversity drives the evolution of CRISPR-based phage resistance. Nature, 574(7779), 549-552.

Antipov, Dmitry, Mikhail Raiko, Alla Lapidus, and Pavel A. Pevzner. "Metaviral SPAdes: assembly of viruses from metagenomic data." Bioinformatics 36, no. 14 (2020): 4126-4129.

Bateman, Alex, Lachlan Coin, Richard Durbin, Robert D. Finn, Volker Hollich, Sam Griffiths-Jones, Ajay Khanna et al. "The Pfam protein families database." *Nucleic acids research* 32, no. suppl_1 (2004): D138-D141.

Bikard, David, Chad W. Euler, Wenyan Jiang, Philip M. Nussenzweig, Gregory W. Goldberg, Xavier Duportet, Vincent A. Fischetti, and Luciano A. Marraffini. "Exploiting CRISPR-Cas nucleases to produce sequence-specific antimicrobials." Nature biotechnology 32, no. 11 (2014): 1146-1150.

Bin Jang, Ho, Benjamin Bolduc, Olivier Zablocki, Jens H. Kuhn, Simon Roux, Evelien M. Adriaenssens, J. Rodney Brister et al. "Taxonomic assignment of uncultivated prokaryotic virus genomes is enabled by gene-sharing networks." *Nature biotechnology* 37, no. 6 (2019): 632-639.

Blazanin, M., & Turner, P. E. (2021). Community context matters for bacteria-phage ecology and evolution. *The ISME Journal*, *15*(11), 3119-3128.

Abramson, Josh, Jonas Adler, Jack Dunger, Richard Evans, Tim Green, Alexander Pritzel, Olaf Ronneberger et al. "Accurate structure prediction of biomolecular interactions with AlphaFold 3." Nature (2024): 1-3.

Berry, Trista M., and Peter J. Christie. "Caught in the act: the dialogue between bacteriophage R17 and the type IV secretion machine of plasmid R1." *Molecular microbiology* 82, no. 5 (2011): 1039-1043.

Bushnell, B. (2020). BBMap. sourceforge.
net/projects/bbmap.https://cir.nii.ac.jp/crid/1370294643771707027

Buttimer, Colin, Tom Sutton, Joan Colom, Ellen Murray, Pedro H. Bettio, Linda Smith, Andrei S. Bolocan et al. "Impact of a phage cocktail targeting Escherichia coli and Enterococcus faecalis as members of a gut bacterial consortium in vitro and in vivo." Frontiers in Microbiology 13 (2022): 936083.

Carlson, H.K., Piya, D., Moore, M.L., Magar, R.T., Elisabeth, N.H., Deutschbauer, A.M., Arkin, A.P. and Mutalik, V.K., 2023. Geochemical constraints on bacteriophage infectivity in terrestrial environments. *ISME communications*, *3*(1), p.78.

Chapman-McQuiston, E., and X. L. Wu. "Stochastic receptor expression allows sensitive bacteria to evade phage attack. Part I: experiments." Biophysical journal 94, no. 11 (2008): 4525-4536.

Chaumeil, Pierre-Alain, Aaron J. Mussig, Philip Hugenholtz, and Donovan H. Parks. "GTDB-Tk: a toolkit to classify genomes with the Genome Taxonomy Database." (2020): 1925-1927.

Chen, LinXing, and Jillian F. Banfield. "COBRA improves the completeness and contiguity of viral genomes assembled from metagenomes." Nature Microbiology 9, no. 3 (2024): 737-750.

Clegg, Tom, and Thilo Gross. "Cross-feeding creates tipping points in microbiome diversity." Proceedings of the National Academy of Sciences 122, no. 19 (2025): e2425603122.

Cole, Benjamin J., Meghan E. Feltcher, Robert J. Waters, Kelly M. Wetmore, Tatiana S. Mucyn, Elizabeth M. Ryan, Gaoyan Wang et al. "Genome-wide identification of bacterial plant colonization genes." PLoS Biology 15, no. 9 (2017): e2002860.

Das, Mayukh, Tushar Suvra Bhowmick, Stephen J. Ahern, Ry Young, and Carlos F. Gonzalez. "Control of Pierce's disease by phage." *PLoS One* 10, no. 6 (2015): e0128902.

Dukovski, Ilija, Djordje Bajić, Jeremy M. Chacón, Michael Quintin, Jean CC Vila, Snorre Sulheim, Alan R. Pacheco et al. "A metabolic modeling platform for the computation of microbial ecosystems in time and space (COMETS)." *Nature protocols* 16, no. 11 (2021): 5030-5082.

Franco Ortega, S., Fields, B., Narino Rojas, D., Mikonranta, L., Holmes, M., Harper, A. L., & Friman, V. P. (2024). Phage biocontrol success of bacterial wilt depends on synergistic interactions with resident rhizosphere microbiota. Microbial Biotechnology, 17(11), e70049.

Finkel, Omri M., Isai Salas-González, Gabriel Castrillo, Jonathan M. Conway, Theresa F. Law, Paulo José Pereira Lima Teixeira, Ellie D. Wilson, Connor R. Fitzpatrick, Corbin D. Jones, and Jeffery L. Dangl. "A single bacterial genus maintains root growth in a complex microbiome." *Nature* 587, no. 7832 (2020): 103-108.

Frias-Lopez, Jorge, Yanmei Shi, Gene W. Tyson, Maureen L. Coleman, Stephan C. Schuster, Sallie W. Chisholm, and Edward F. DeLong. "Microbial community gene expression in ocean surface waters." Proceedings of the National Academy of Sciences 105, no. 10 (2008): 3805-3810.

Friedman, Jonathan, and Eric J. Alm. "Inferring correlation networks from genomic survey data." (2012): e1002687.

Gao, Chun-Hui, Hui Cao, Peng Cai, and Søren J. Sørensen. "The initial inoculation ratio regulates bacterial coculture interactions and metabolic capacity." *The ISME journal* 15, no. 1 (2021): 29-40.

Gilbert, Jack A., Dawn Field, Ying Huang, Rob Edwards, Weizhong Li, Paul Gilna, and Ian Joint. "Detection of large numbers of novel sequences in the metatranscriptomes of complex marine microbial communities." *PloS one* 3, no. 8 (2008): e3042.

Goldford, Joshua E., Nanxi Lu, Djordje Bajić, Sylvie Estrela, Mikhail Tikhonov, Alicia Sanchez-Gorostiaga, Daniel Segrè, Pankaj Mehta, and Alvaro Sanchez. "Emergent simplicity in microbial community assembly." Science 361, no. 6401 (2018): 469-474.

Gencay, Y.E., Jasinskytė, D., Robert, C., Semsey, S., Martínez, V., Petersen, A.Ø., Brunner, K., de Santiago Torio, A., Salazar, A., Turcu, I.C. and Eriksen, M.K., 2024. Engineered phage with antibacterial CRISPR–Cas selectively reduce E. coli burden in mice. Nature Biotechnology, 42(2), pp.265-274.

Han, Jong-In, Hong-Kyu Choi, Seung-Won Lee, Paul M. Orwin, Jina Kim, Sarah L. LaRoe, Tae-gyu Kim et al. "Complete genome sequence of the metabolically versatile plant growth-promoting endophyte Variovorax paradoxus S110." *Journal of bacteriology* 193, no. 5 (2011): 1183-1190.

Hessler, Tomas, Robert J. Huddy, Rohan Sachdeva, Shufei Lei, Susan TL Harrison, Spencer Diamond, and Jillian F. Banfield. "Vitamin interdependencies predicted by metagenomics-informed network analyses and validated in microbial community microcosms." Nature Communications 14, no. 1 (2023): 4768.

Hyatt, Doug, Gwo-Liang Chen, Philip F. LoCascio, Miriam L. Land, Frank W. Larimer, and Loren J. Hauser. "Prodigal: prokaryotic gene recognition and translation initiation site identification." *BMC bioinformatics* 11 (2010): 1-11.

Igler, C., 2022. Phenotypic flux: The role of physiology in explaining the conundrum of bacterial persistence amid phage attack. *Virus evolution*, *8*(2), p.veac086.

Johnson, Christopher M., M. Michael Harden, and Alan D. Grossman. "Interactions between mobile genetic elements: An anti-phage gene in an integrative and conjugative element protects host cells from predation by a temperate bacteriophage." PLoS Genetics 18, no. 2 (2022): e1010065.

Joshi, N. A.; Fass, J. N. (**2011**). *Sickle: A sliding-window, adaptive, quality-based trimming tool for FastQ files*. (Version 1.33) [Software], https://github.com/najoshi/sickle.

Kamruzzaman, Muhammad, Amy J. Mathers, and Jonathan R. Iredell. "A Novel Plasmid Entry Exclusion System in pKPC_UVA01, a Promiscuous Conjugative Plasmid Carrying the bla KPC Carbapenemase Gene." Antimicrobial Agents and Chemotherapy 66, no. 3 (2022): e02322-21.

Kanehisa, M., & Goto, S. (2000). KEGG: kyoto encyclopedia of genes and genomes. *Nucleic acids research*, *28*(1), 27-30.

Kang, F. Li, E. Kirton, A. Thomas, R. Egan, H. An, Z. Wang, MetaBAT 2: an adaptive binning algorithm for robust and efficient genome reconstruction from metagenome assemblies. PeerJ 7, e7359 (2019).

Kost, Christian, Kiran Raosaheb Patil, Jonathan Friedman, Sarahi L. Garcia, and Markus Ralser. "Metabolic exchanges are ubiquitous in natural microbial communities." Nature Microbiology 8, no. 12 (2023): 2244-2252.

Kliem, Manfred, and Brigitte Dreiseikelmann. "The superimmunity gene sim of bacteriophage P1 causes superinfection exclusion." *Virology* 171, no. 2 (1989): 350-355.

Kust, Andreja, Jackie Zorz, Catalina Cruañas Paniker, Keith Bouma-Gregson, Netravathi Krishnappa, Jillian F. Banfield, and Spencer Diamond. "Model cyanobacterial consortia reveal a consistent core microbiome independent of inoculation source or cyanobacterial host species." bioRxiv (2023): 2023-12.

Langmead, Ben, and Steven L. Salzberg. "Fast gapped-read alignment with Bowtie 2." *Nature methods* 9, no. 4 (2012): 357-359.

Li, Y., Zhu, F., Li, Y., Pan, S., Wang, H., Yang, Z., ... & Liu, B. (2022). Bacteriophages allow selective depletion of gut bacteria to produce a targeted-bacterium-depleted mouse model. *Cell Reports Methods*, *2*(11).

Li, Yang Grace, and Peter J. Christie. "The Agrobacterium VirB/VirD4 T4SS: mechanism and architecture defined through in vivo mutagenesis and chimeric systems." *Agrobacterium Biology: From Basic Science to Biotechnology* (2018): 233-260.

Liao, H., Wen, C., Huang, D., Liu, C., Gao, T., Du, Q., ... & Friman, V. P. (2025). Harnessing phage consortia to mitigate the soil antibiotic resistome by targeting keystone taxa Streptomyces. *Microbiome*, *13*(1), 1-20.

Ma, Bin, Yiling Wang, Shudi Ye, Shan Liu, Erinne Stirling, Jack A. Gilbert, Karoline Faust et al. "Earth microbial co-occurrence network reveals interconnection pattern across microbiomes." *Microbiome* 8, no. 1 (2020): 1-12.

Mutalik, V. K., Adler, B. A., Rishi, H. S., Piya, D., Zhong, C., Koskella, B., ... & Arkin, A. P. (2020). High-throughput mapping of the phage resistance landscape in E. coli. *PLoS biology*, *18*(10), e3000877.

Nissen, Jakob Nybo, Joachim Johansen, Rosa Lundbye Allesøe, Casper Kaae Sønderby, Jose Juan Almagro Armenteros, Christopher Heje Grønbech, Lars Juhl Jensen et al. "Improved metagenome binning and assembly using deep variational autoencoders." *Nature biotechnology* 39, no. 5 (2021): 555-560.

Oksanen, G. L. Simpson, F. G. Blanchet, R. Kindt, P. Legendre, P. R. Minchin, R. B. O'Hara, P. Solymos, M. H. H. Stevens, E. Szoecs, H. Wagner, M. Barbour, M. Bedward, B. Bolker, D. Borcard, G. Carvalho, M. Chirico, M. De Caceres, S. Durand, H. B. A. Evangelista, R. FitzJohn, M. Friendly, B. Furneaux, G. Hannigan, M. O. Hill, L. Lahti, D. McGlinn, M.-H. Ouellette, E. Ribeiro Cunha, T. Smith, A. Stier, C. J. F. Ter Braak, J. Weedon, vegan: Community Ecology Package, (2001); https://doi.org/10.32614/CRAN.package.vegan.

Olm, Matthew R., Christopher T. Brown, Brandon Brooks, and Jillian F. Banfield. "dRep: a tool for fast and accurate genomic comparisons that enables improved genome recovery from metagenomes through de-replication." *The ISME journal* 11, no. 12 (2017): 2864-2868.

Olm, Matthew R., Alexander Crits-Christoph, Keith Bouma-Gregson, Brian A. Firek, Michael J. Morowitz, and Jillian F. Banfield. "inStrain profiles population microdiversity from metagenomic data and sensitively detects shared microbial strains." *Nature Biotechnology* 39, no. 6 (2021): 727-736.

Pacheco, Alan R., and Daniel Segrè. "A multidimensional perspective on microbial interactions." FEMS microbiology letters 366, no. 11 (2019): fnz125.

Pacesa, M., Nickel, L., Schellhaas, C., Schmidt, J., Pyatova, E., Kissling, L., Barendse, P., Choudhury, J., Kapoor, S., Alcaraz-Serna, A. and Cho, Y., 2024. BindCraft: one-shot design of functional protein binders. bioRxiv, pp.2024-09.

Payne L.J., Meaden S., Mestre M.R., Palmer C., Toro N., Fineran P.C. and Jackson S.A.* (2022) PADLOC: a web server for the identification of antiviral defence systems in microbial genomes. Nucleic Acids Research 50, W541-W550. doi: 10.1093/nar/gkac400

Peng, Yu, Henry CM Leung, Siu-Ming Yiu, and Francis YL Chin. "IDBA-UD: a de novo assembler for single-cell and metagenomic sequencing data with highly uneven depth." Bioinformatics 28, no. 11 (2012): 1420-1428.

Pierce, Emily C., and Rachel J. Dutton. "Putting microbial interactions back into community contexts." *Current Opinion in Microbiology* 65 (2022): 56-63.

Pirnay, Jean-Paul, Sarah Djebara, Griet Steurs, Johann Griselain, Christel Cochez, Steven De Soir, Tea Glonti et al. "Personalized bacteriophage therapy outcomes for 100 consecutive cases: a multicentre, multinational, retrospective observational study." Nature Microbiology (2024): 1-20.

Pyenson, N.C., Leeks, A., Nweke, O., Goldford, J.E., Schluter, J., Turner, P.E., Foster, K.R. and Sanchez, A., 2024. Diverse phage communities are maintained stably on a clonal bacterial host. *Science*, *386*(6727), pp.1294-1300.

Quinn-Bohmann, Nick, Tomasz Wilmanski, Katherine Ramos Sarmiento, Lisa Levy, Johanna W. Lampe, Thomas Gurry, Noa Rappaport et al. "Microbial community-scale metabolic modelling predicts personalized short-chain fatty acid production profiles in the human gut." *Nature Microbiology* 9, no. 7 (2024): 1700-1712.

Quinones-Olvera, Natalia, Siân V. Owen, Lucy M. McCully, Maximillian G. Marin, Eleanor A. Rand, Alice C. Fan, Oluremi J. Martins Dosumu et al. "Diverse and abundant phages exploit conjugative plasmids." Nature Communications 15, no. 1 (2024): 3197.

Ram, Rachna J., Nathan C. VerBerkmoes, Michael P. Thelen, Gene W. Tyson, Brett J. Baker, Robert C. Blake, Manesh Shah, Robert L. Hettich, and Jillian F. Banfield. "Community proteomics of a natural microbial biofilm." *Science* 308, no. 5730 (2005): 1915-1920.

Ramirez, Jaime, Francisco guarner, Luis Bustos Fernandez, Aldo Maruy, Vera Lucia Sdepanian, and Henry Cohen. "Antibiotics as major disruptors of gut microbiota." Frontiers in cellular and infection microbiology 10 (2020): 572912.

Redzej, Adam, Marta Ukleja, Sarah Connery, Martina Trokter, Catarina Felisberto-Rodrigues, Adam Cryar, Konstantinos Thalassinos, Richard D. Hayward, Elena V. Orlova, and Gabriel Waksman. "Structure of a VirD4 coupling protein bound to a VirB type IV secretion machinery." *The EMBO journal* 36, no. 20 (2017): 3080-3095.

Rivard, Nicolas, Malika Humbert, Kévin T. Huguet, Aurélien Fauconnier, César Pérez Bucio, Eve Quirion, and Vincent Burrus. "Surface exclusion of IncC conjugative plasmids and their relatives." Plos Genetics 20, no. 10 (2024): e1011442.

Russell, Marjorie. "Moving through the membrane with filamentous phages." *Trends in microbiology* 3, no. 6 (1995): 223-228.

Aroney S.T.N.(1), Rhys J. P. Newell (1), Jakob N. Nissen (2), Antonio Pedro Camargo (3 and 4), Gene W. Tyson (1), Ben J. Woodcroft. (2025). CoverM: Read alignment statistics for metagenomics. https://doi.org/10.48550/arXiv.2501.11217

Segata, Nicola, Daniela Boernigen, Timothy L. Tickle, Xochitl C. Morgan, Wendy S. Garrett, and Curtis Huttenhower. "Computational meta'omics for microbial community studies." *Molecular systems biology* 9, no. 1 (2013): 666.

Schenk, Hanna, and Michael Sieber. "Bacteriophage can promote the emergence of physiologically sub-optimal host phenotypes." bioRxiv (2019): 621524.

Selle, K., Fletcher, J.R., Tuson, H., Schmitt, D.S., McMillan, L., Vridhambal, G.S., Rivera, A.J., Montgomery, S.A., Fortier, L.C., Barrangou, R. and Theriot, C.M., 2020. In vivo targeting of Clostridioides difficile using phage-delivered CRISPR-Cas3 antimicrobials. MBio, 11(2), pp.10-1128.

Skwara, Abigail, Karna Gowda, Mahmoud Yousef, Juan Diaz-Colunga, Arjun S. Raman, Alvaro Sanchez, Mikhail Tikhonov, and Seppe Kuehn. "Statistically learning the functional landscape of microbial communities." Nature ecology & evolution 7, no. 11 (2023): 1823-1833.

Starr, Evan P., Shengjing Shi, Steven J. Blazewicz, Alexander J. Probst, Donald J. Herman, Mary K. Firestone, and Jillian F. Banfield. "Stable isotope informed genome-resolved metagenomics reveals that Saccharibacteria utilize microbially-processed plant-derived carbon." *Microbiome* 6 (2018): 1-12

Strathdee, Steffanie A., Graham F. Hatfull, Vivek K. Mutalik, and Robert T. Schooley. "Phage therapy: From biological mechanisms to future directions." Cell 186, no. 1 (2023): 17-31.

Sieber, Christian MK, Alexander J. Probst, Allison Sharrar, Brian C. Thomas, Matthias Hess, Susannah G. Tringe, and Jillian F. Banfield. "Recovery of genomes from metagenomes via a dereplication, aggregation and scoring strategy." *Nature microbiology* 3, no. 7 (2018): 836-843.

Taylor, Véronique L., Megha Shah, Pramalkumar H. Patel, Ahmed Yusuf, Cayla M. Burk, Zemer Gitai, Alan R. Davidson, Matthias D. Koch, and Karen L. Maxwell. "Prophages block cell surface receptors to ensure survival of their viral progeny." bioRxiv (2024): 2024-03.

Thanki, Anisha M., Guillaume Mignard, Robert J. Atterbury, Paul Barrow, Andrew D. Millard, and Martha RJ Clokie. "Prophylactic delivery of a bacteriophage cocktail in feed significantly reduces Salmonella colonization in pigs." Microbiology spectrum 10, no. 3 (2022): e00422-22.

Thorgersen, M.P., Xue, J., Majumder, E.L., Trotter, V.V., Ge, X., Poole, F.L., Owens, T.K., Lui, L.M., Nielsen, T.N., Arkin, A.P. and Deutschbauer, A.M., 2021. Deciphering microbial metal toxicity responses via random bar code transposon site sequencing and activity-based metabolomics. Applied and environmental microbiology, 87(21), pp.e01037-21.

Trgovec-Greif, Lovro, Hans-Jörg Hellinger, Jean Mainguy, Alexander Pfundner, Dmitrij Frishman, Michael Kiening, Nicole Suzanne Webster, Patrick William Laffy, Michael Feichtinger, and Thomas Rattei. "VOGDB—database of virus orthologous groups." *Viruses* 16, no. 8 (2024): 1191.

Tyson, Gene W., Jarrod Chapman, Philip Hugenholtz, Eric E. Allen, Rachna J. Ram, Paul M. Richardson, Victor V. Solovyev, Edward M. Rubin, Daniel S. Rokhsar, and Jillian F. Banfield. "Community structure and metabolism through reconstruction of microbial genomes from the environment." *Nature* 428, no. 6978 (2004): 37-43.

Watts, Mathew P., Liam P. Spurr, Kim-Anh Lê Cao, Ryan Wick, Jillian F. Banfield, and John W. Moreau. "Genome-resolved metagenomics of an autotrophic thiocyanate-remediating microbial bioreactor consortium." Water research 158 (2019): 106-117.

Watts, Stephen C., Scott C. Ritchie, Michael Inouye, and Kathryn E. Holt. "FastSpar: rapid and scalable correlation estimation for compositional data." *Bioinformatics* 35, no. 6 (2019): 1064-1066.

Wang, Xiaofang, Shuo Wang, Mingcong Huang, Yilin He, Saisai Guo, Keming Yang, Ningqi Wang et al. "Phages enhance both phytopathogen density control and rhizosphere microbiome suppressiveness." Mbio 15, no. 6 (2024): e03016-23.

Wang, Xiaofang, Zhong Wei, Keming Yang, Jianing Wang, Alexandre Jousset, Yangchun Xu, Qirong Shen, and Ville-Petri Friman. "Phage combination therapies for bacterial wilt disease in tomato." *Nature Biotechnology* 37, no. 12 (2019): 1513-1520.

Wetmore, Kelly M., Morgan N. Price, Robert J. Waters, Jacob S. Lamson, Jennifer He, Cindi A. Hoover, Matthew J. Blow et al. "Rapid quantification of mutant fitness in diverse bacteria by sequencing randomly bar-coded transposons." *MBio* 6, no. 3 (2015): 10-1128.

Wu Y.-W. , B. A. Simmons, S. W. Singer, MaxBin 2.0: an automated binning algorithm to recover genomes from multiple metagenomic datasets. Bioinformatics 32, 605–607 (2016).

Yoo, Seongjun, Kang-Mu Lee, Nayoung Kim, Thao Nguyen Vu, Ricardo Abadie, and Dongeun Yong. "Designing phage cocktails to combat the emergence of bacteriophage-resistant mutants in multidrug-resistant Klebsiella pneumoniae." Microbiology spectrum 12, no. 1 (2024): e01258-23.

Zielezinski, Andrzej, Adam Gudys, Jakub Barylski, Krzysztof Siminski, Piotr Rozwalak, Bas E. Dutilh, and Sebastian Deorowicz. "Ultrafast and accurate sequence alignment and clustering of viral genomes." *bioRxiv* (2024): 2024-06.

Supplementary materials

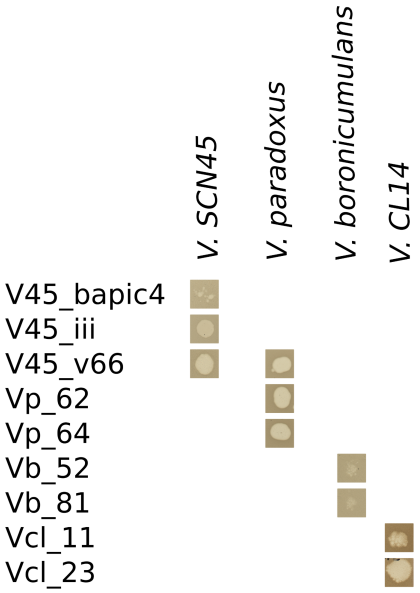

Figure S1. Plaque morphology from spot assays performed on *Variovorax* species with the nine isolated *Variovorax* phages. Only phage V45_66 was able to plaque on more than one host.

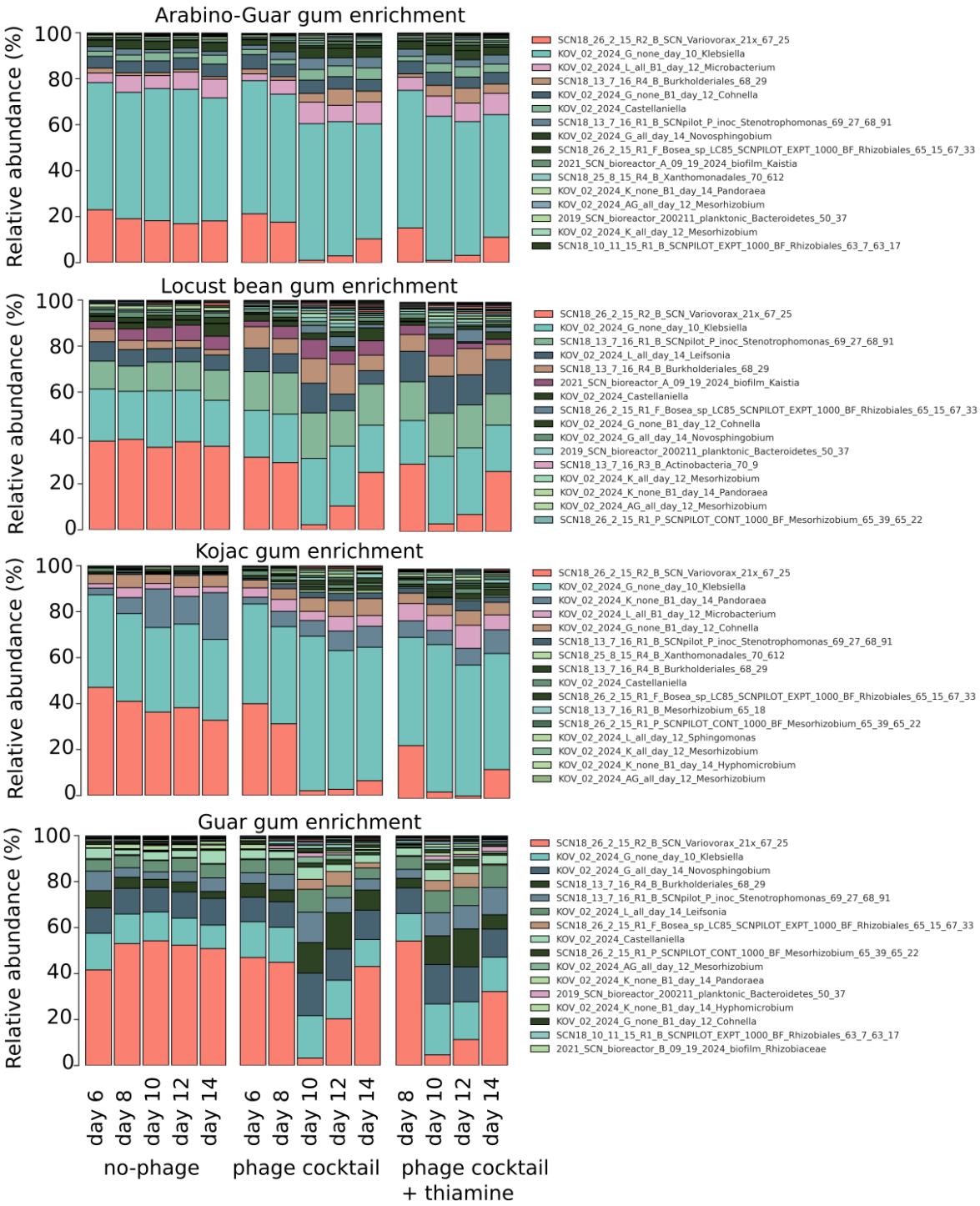

Figure S2. Genome-resolved metagenomics reveals consistent reduction in the relative abundance in Variovorax across all four enrichment cultures following phage application. The 16 most abundant organisms per enrichment culture recovered are shown.

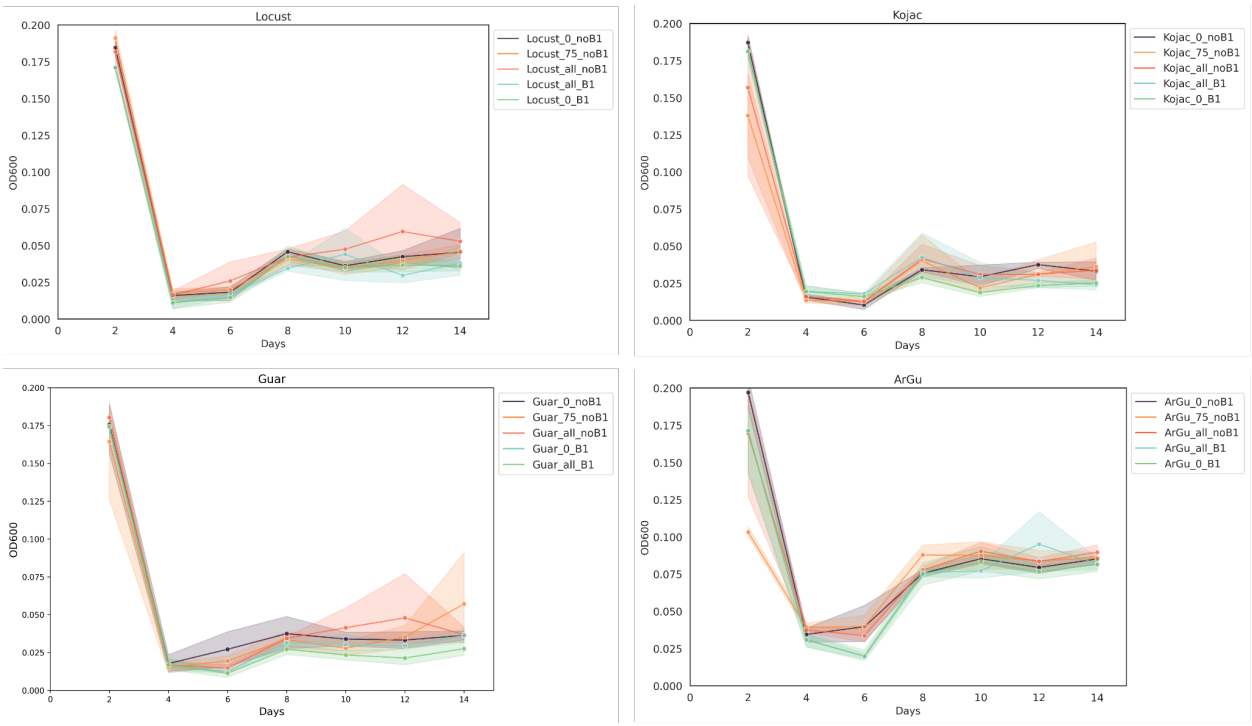

Figure S3. The optical density (600nm) of the 48 hour old communities following inoculation and each subsequent passage. All communities show a sharp reduction between day 2 and day 4 communities but then reach a stable state from day eight onwards.

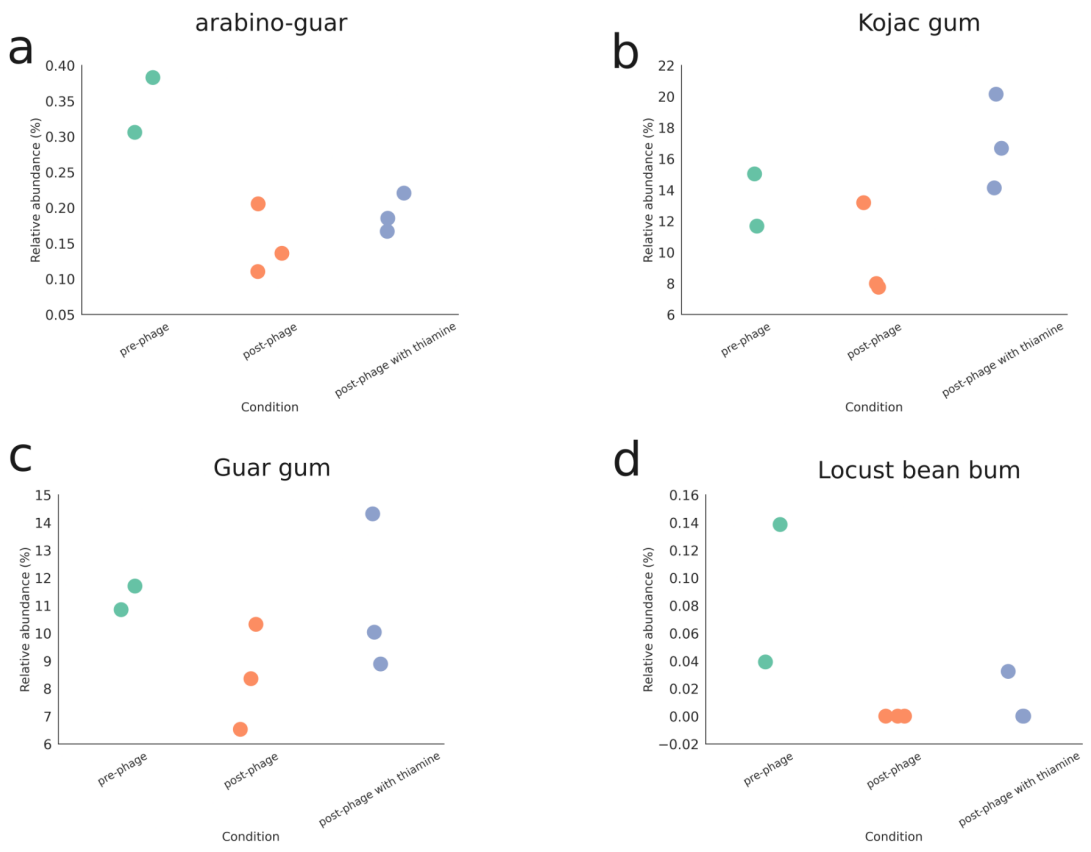

Figure S4. *Leifsonia* MAG relative abundance is consistent with the ASV data. The abundance of this MAG is shown across the four carbon source enrichment cultures before phage addition (day 6 and day 8 communities), following phage infection (day 10, day 12, day 14 communities), and following phage infection with supplementation of thiamine.

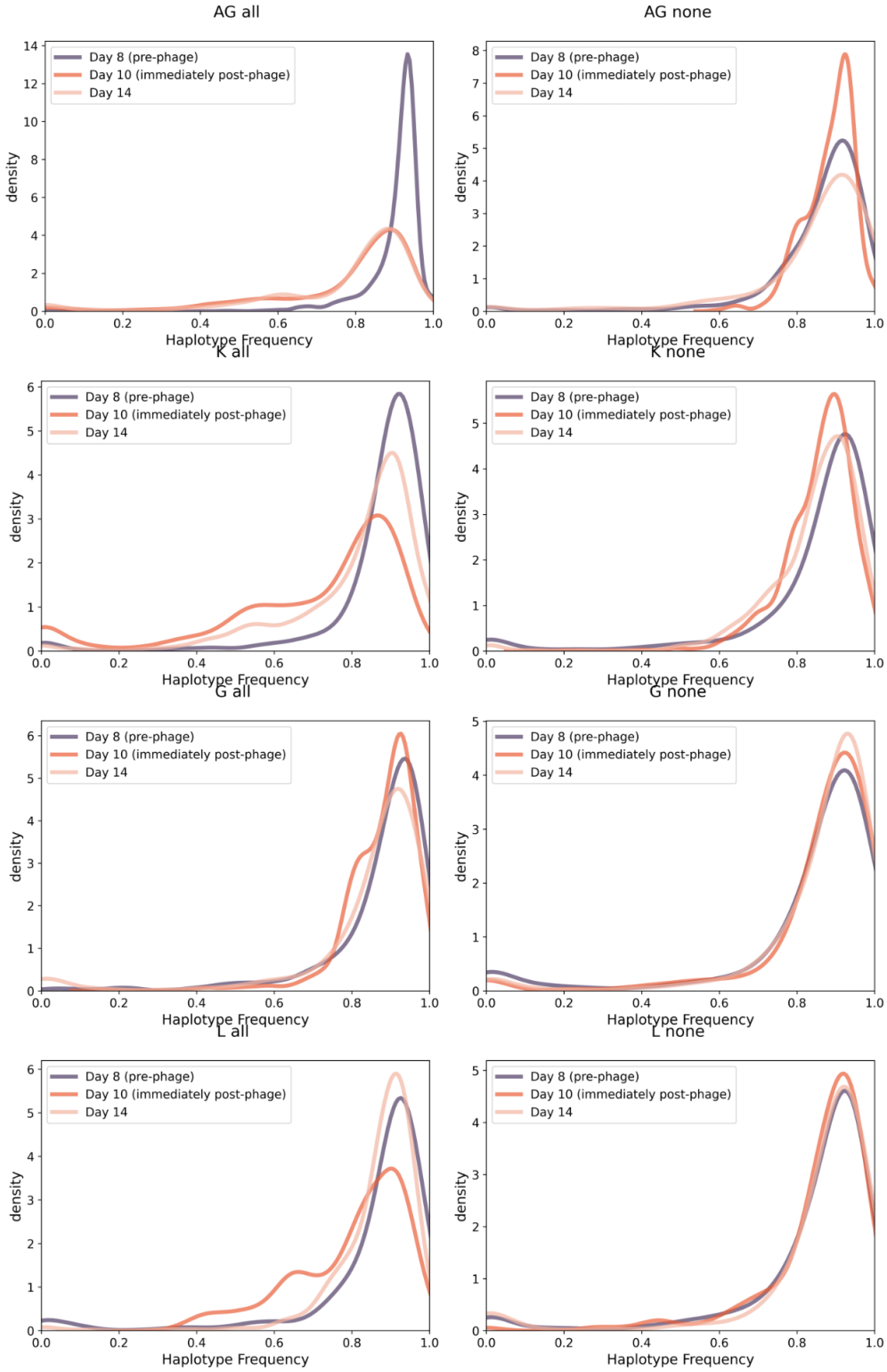

Figure S5. Haplotype frequencies associated with phage exposure to each of the four enrichment communities and their no-phage controls.

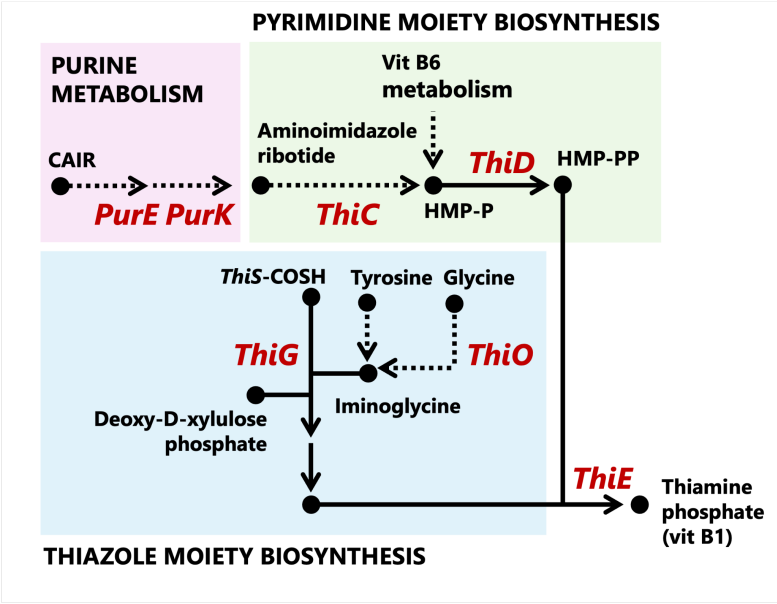

Figure S6. Thiamine biosynthesis pathway illustrating the multiple routes for the production of the thiazole and pyrimidine moieties of thiamine. Adapted from https://www.kegg.jp/ (Kanehisa & Goto, 2000).